

# THE ASTROPHYSICAL JOURNAL

AN INTERNATIONAL REVIEW OF SPECTROSCOPY AND  
ASTRONOMICAL PHYSICS

VOLUME LXVI

JULY 1927

NUMBER 1

## THE CHROMOSPHERIC SPECTRUM AS OBSERVED WITH AN OBJECTIVE PRISM AT THE ECLIPSE OF JANUARY 24, 1925

By G. F. PADDOCK

### ABSTRACT

At the moment of central phase a photograph of the spectrum of the chromosphere was secured with an 8-inch  $15^\circ$  prism in front of the 12-inch lens of the 15-foot refractor of Ladd Observatory. The *spectral arcs* shown on the negative are *identified* with the principal chromospheric lines. From the measured *angular extent of the arcs* are computed the *apparent heights* of the radiating gases. The *northern edge of the shadow* passed three-quarters of a mile (1.2 km) *south* of the Observatory. The minimum width of crescent was 0".8, corresponding to one and a half seconds of time before totality on the central line. The difference between the *centers of the sun and moon* was derived from the plate, giving a *correction to the almanac value* of the moon's declination of  $\Delta\delta = +0".85$ .

The hydrogen arcs observed on the photograph show the usual definite decrease in length and intensity from  $H_\alpha$  toward the violet. If at the time of such an observation provision were made for the photometric measurement of the gradients of line-intensities and the ratios of intensity in the series lines, the data derived would aid in the study of the physical condition of the chromosphere and its radiation.

Observation at the edge of the path of the shadow has the advantage of longer time for exposures and of securing the full lengths of spectral arcs.

The shadow of the total eclipse of the sun of January 24, 1925, was predicted to pass over the city of Providence, Rhode Island. Its northern edge would lie only a short distance south of the Ladd Observatory of Brown University at Providence. This circumstance offered opportunity for observation of the solar chromosphere by means of an objective prism in connection with the 12-inch refractor of the Observatory. The spectrum of the chromosphere, usually referred to as the "flash" or "emission" spectrum, has been observed most frequently at positions on or near the central line of the path of the shadow at beginning and ending of totality when the appearance of the bright lines is only momentary. It has been observed

also both inside and outside of the shadow during the partial phases by adjusting the slit of a spectroscope or spectrograph tangent to the cusp of the sun's crescent so that it may receive the chromospheric light extending beyond the point of the photospheric crescent. Near the edge of the shadow the bright spectrum is available for study or exposure for an interval extending toward half an hour. At the edge of the shadow as the moon's limb grazes the sun's limb there is an interval of several seconds during which a long arc of the chromosphere is visible and available for exposure. A photograph with an objective prism of this chromospheric arc presents a series of arcs corresponding to monochromatic lines of the spectrum of the luminous gases of the chromosphere. If the observer is just outside the shadow, so that a short limb of the sun remains uncovered, the continuous spectrum of the photospheric light is also recorded on the photograph and appears as a black band lying across the spectrum arcs in the direction of the dispersion. Observations of this sort were made of the solar eclipse of 1905 in Algeria by Mr. John Evershed<sup>1</sup> under circumstances similar to those at Providence. The occurrence of an eclipse shadow passing close to an established observatory as at Providence in 1925 is unusual. The results derived from the event are here presented.

#### EQUIPMENT, ADJUSTMENTS, AND PROCEDURE

The Ladd Observatory is located in latitude  $41^{\circ} 50' 21''$  and longitude  $4^{\text{h}} 45^{\text{m}} 35^{\text{s}}.95$  west of Greenwich at an elevation of 64 m. Its telescope has a Brashear objective of 12.2 inches (310 mm) aperture and 15.1 feet (460 cm) focal length. The prism used at this time was offered by Dr. Shapley from the equipment of Harvard College Observatory, for which acknowledgment is here made. It has an aperture of 8 inches (20.3 cm) and an angle of  $15^{\circ}$ . By means of its circular brass cell and a provisional frame of wood, it was firmly fixed over the objective with the refracting edge perpendicular to a meridional plane. A camera belonging to the telescope was adjusted to the solar focus and the guiding telescope set for properly directing the large telescope on the sun. Wratten and Wainwright panchromatic plates 4 by 5 inches in size were used. Exposures of about one

<sup>1</sup> *Monthly Notices of the Royal Astronomical Society*, Appendix, 60, 34, 1900.

second were made by drawing the slide. The apparatus had no shutter for exact timing, and no knowledge of the necessary exposure time was available. During the interval from several minutes before until several minutes after the computed time of maximum phase a series of exposures was made, with the intent of catching the bright spectrum with the least continuous spectrum from the uncovered limb. Mr. William T. Grinnell, assistant at the Observatory, very generously assisted in all the preliminary work and the observations.

#### ECLIPSE DATA

The time of first contact, computed to be  $8^{\text{h}} 3^{\text{m}} 7^{\text{s}}$  A.M., E.S.T., was observed to be  $8^{\text{h}} 3^{\text{m}} 20^{\text{s}}$ . The time of central phase, of course, could not be exactly noted but seemed to be identical with that computed, namely, seventy-fifth meridian time  $9^{\text{h}} 15^{\text{m}} 33^{\text{s}}$ . The last contact, computed to be  $10^{\text{h}} 34^{\text{m}} 50^{\text{s}}$ , was observed at  $10^{\text{h}} 34^{\text{m}} 30^{\text{s}}$ . The direction of the path of the shadow was from  $16^{\circ}$  north of the west point to  $16^{\circ}$  south of the east point. The altitude of the sun given by the apparent time of the observation was  $18^{\circ} 18'$ . The computed magnitude of the eclipse was 0.99969, giving a minimum width of the crescent of 0'.6 and indicating that the edge of the shadow would lie about a mile southward from the Observatory. The sky on the night preceding the eclipse was brilliantly clear with a very cold northwest wind and minimum temperature of  $-1^{\circ}$  F. At the time of the eclipse the temperature was  $+6^{\circ}$  F. The eastern sky presented a slightly hazy appearance with some areas of thin clouds south and west of the zenith. During the moment of greatest obscuration the short bright arc of the sun's limb, still visible, rapidly shifted around a considerable extent of the northerly limb of the moon, and it was during this interval that the bright lines of the chromospheric spectrum were recorded on three of the plates exposed, one of which is here described and reproduced. During this interval, also, the corona around the dark contour of the moon was faintly seen and noted by Mr. Carl Whitier, a student-observer present for the visual observation and recording of contact times.

#### NEGATIVES AND MEASUREMENTS

The three negatives which show the bright lines have the black band due to continuous spectrum of the limb situated differently

with respect to the arcs. On the plate showing the arcs nearly perpendicular to the band their positions for identification were measured with a Gaertner measuring-machine. The linear dispersion shown by the spectrum varies from about 25 Å to the millimeter at 3800 Å to 37 at  $H\gamma$  and 150 at  $H\alpha$ . Measurement could give only a very rough determination of wave-lengths. Under the microscope the images are mere shadows and only the brightest and strongest lines are seen. Sharp narrow lines or good definition could hardly be expected with the uncertain focus and unsteadiness of the images, or with so long a focal length of objective and so great effective width of slit or source of light as was presented by the limb and chromosphere of the sun. However, the hydrogen lines from  $H\alpha$  to  $H\theta$  are certainly identifiable, and from a plot of the settings on all the lines, or appearances of lines, against the hydrogen wave-lengths, the approximate wave-lengths of the other lines were derived and found to correspond with the stronger lines in S. A. Mitchell's list<sup>1</sup> observed in 1905. The lines thus identified are given in Table I. The order of strength of these lines is indicated in the third column, and the figures are given in two unrelated systems because the lines of hydrogen are very much stronger than the other lines.

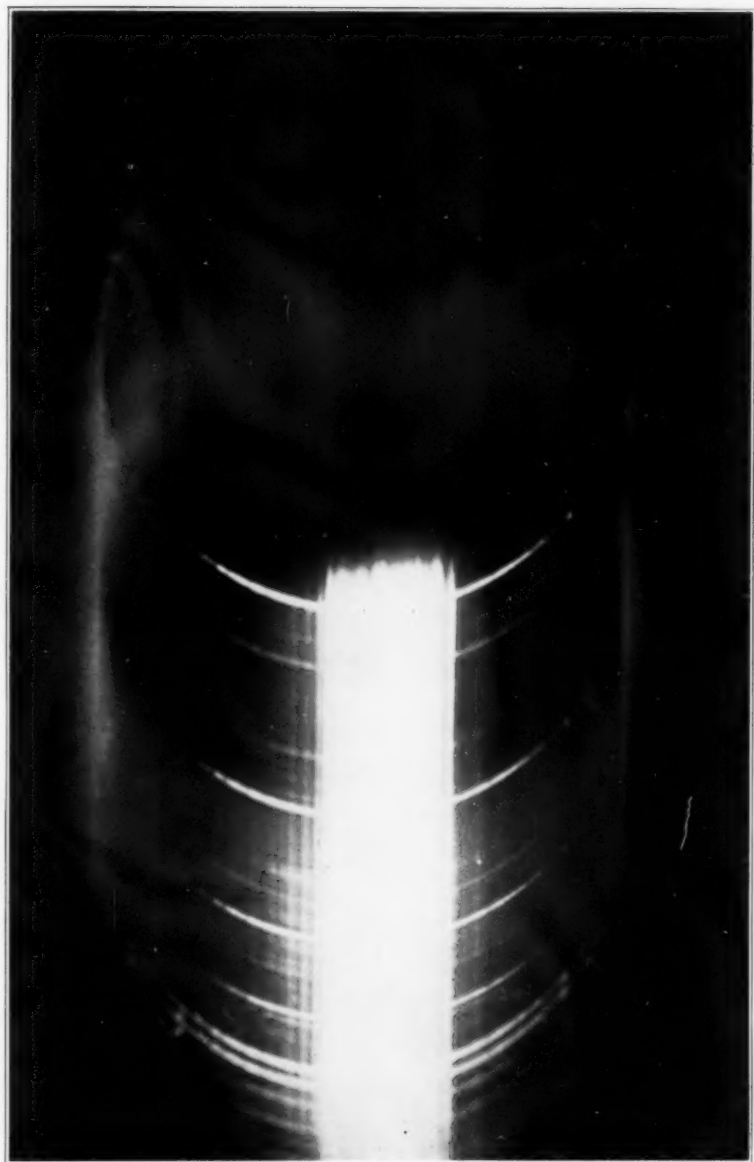
Plate I is a reproduction of the negative showing the longest arcs. The stronger arcs on this negative present the appearance of a series of overlapping rings, the strongest and most complete being the H and K of calcium and the  $H\alpha$  of hydrogen. Many prominences are indicated by knots along the outer parts of the arcs of calcium, hydrogen, and helium. The dimmer sides of these rings must have their source at considerable heights in the chromosphere. One faint ring plainly seen on the negative, but hardly visible in the reproduction, is very broad and diffuse, covering at least 400 Å in the region 4400–4800 Å. The height of this would seem to reach into the lower coronal regions, and it may be the strong portion of the continuous spectrum of the corona.

The angular extent of the arcs was derived by measuring the chord of each arc with a millimeter scale. The half-angle of the arc is then equal to the arcsine of the ratio of chord to the diameter of the moon's image. This diameter is obtained by measuring the in-

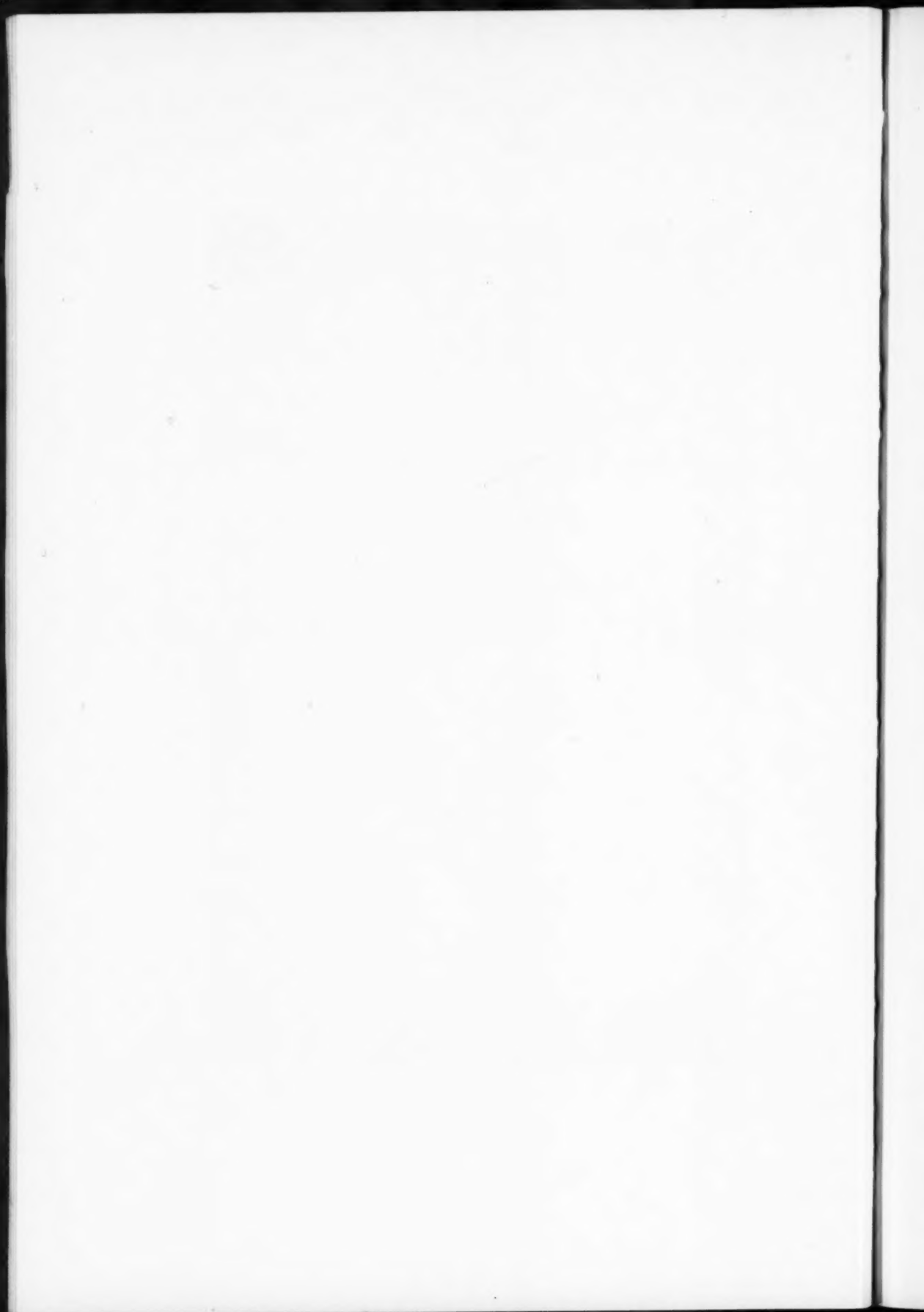
<sup>1</sup> *Astrophysical Journal*, 38, 424, 1913.



PLATE I



THE SPECTRUM OF THE CHROMOSPHERE, JANUARY 24, 1925  
Taken with Objective Prism at Ladd Observatory, Providence, Rhode Island



terior diameter of the full rings given by the strongest lines. That of *Ha* gives 45 mm. The resulting values in degrees are given in the fourth column of Table I. From these angles the heights of chromospheric strata represented by the tips of the arcs were computed and are given in seconds of arc and in kilometers in the fifth column.

TABLE I

Wave-Length	Elements	Intensity	Arc-Length	Height		Remarks
					km	
3760.....	<i>Ti</i>	1	33.7	3.9	2800	
3770.....	<i>H<math>\epsilon</math></i>					
3790.....	<i>H<math>\theta</math></i>	3	33.7	3.9	2800	
3850.....	<i>H<math>\eta</math>, Mg</i>	4	35.3	4.3	3100	
3889.....	<i>H<math>\zeta</math>, Fe</i>	4	38.5	5.2	3700	
3933.....	<i>K, Ca</i>		60.1	13.1	9400	Very strong
3968.....	<i>H, Ca, H<math>\epsilon</math></i>		60.1	13.1	9400	Very strong
4026.....	<i>He</i>	1	30.7	3.1	2200	Faint
4077.....	<i>Sr</i>	10	32.2	3.5	2500	
4101.....	<i>H<math>\delta</math></i>	7	40.1	5.8	4100	Strong
4172.....	<i>Ti</i>	1	23.6	1.5	1100	Faint
4215.....	<i>Sr</i>	7	30.7	3.1	2200	
4226.....	<i>Ca</i>	2	23.6	1.5	1100	
4247.....	<i>Sc</i>	5	26.4	2.1	1500	
4274.....	<i>Cr</i>	3	23.6	1.5	1100	
4290.....	<i>Ca, Cr, Ti</i>	3	23.6	1.5	1100	
4308.....	<i>Ca</i>	2	23.6	1.5	1100	
4340.....	<i>H<math>\gamma</math></i>	8	45.3	7.5	5300	Strong
4374.....	<i>Sc</i>	3	25.0	1.8	1300	
4395.....	<i>Ti</i>	4	25.0	1.8	1300	
4417.....	<i>Ti</i>	3	25.0	1.8	1300	
4455.....	<i>Ca</i>	4	25.0	1.8	1300	
4471.....	<i>He</i>	8	45.3	7.5	5300	
4515.....	<i>Fe</i>	4	26.4	2.1	1500	
4550.....	<i>Ti, Fe, Ba</i>	3	26.4	2.1	1500	
4572.....	<i>Ti</i>	8	26.4	2.1	1500	
4861.....	<i>H<math>\beta</math></i>	9	49.1	8.8	6300	Strong
4924.....	<i>Fe</i>	3	23.6	1.5	1100	
5018.....	<i>Fe</i>	2	23.6	1.5	1100	
5172, 83.....	<i>Mg</i>	9	26.4	2.1	1500	
5875.....	<i>He</i>	10	45.3	7.5	5300	
6562.....	<i>Ha</i>	10	49.1	8.8	6300+	Strong; full ring traceable

On this plate also was measured the width of the band due to the continuous spectrum of the uncovered limb of the sun. This band lies nearly central across the arcs and its width, 11 mm, represents the chord of the lunar and solar arcs of the crescent which, as above, are twice the arcsine of the ratio of chord to the diameters of the lunar and solar images on the negative. Since the solar image

is obscured by the lunar, its diameter must be derived from the lunar by means of the ratio of computed apparent semi-diameters. The width of the crescent is then the difference of the sagittae which follow from the derived arcs.

#### DIAGRAM, NOTATION, AND FORMULAE

The accompanying diagram (Fig. 1) represents the relative positions of the sun and moon or their images on a negative at the mo-

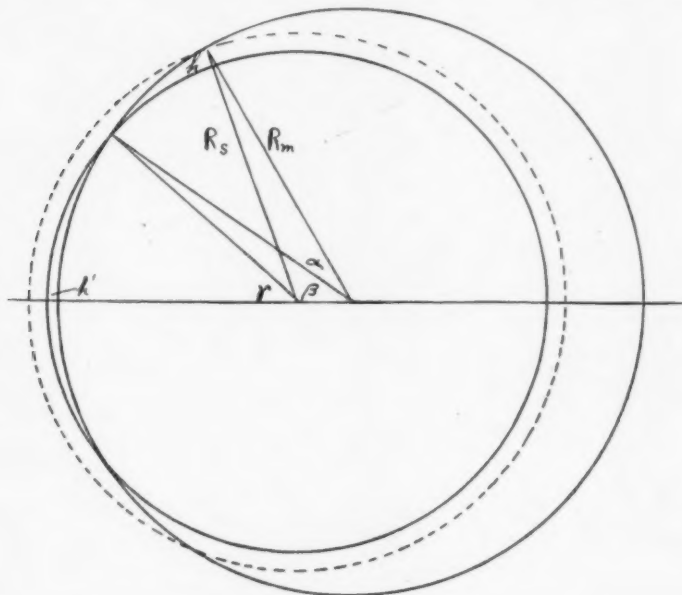


FIG. 1.—Relative positions of sun and moon at moment of exposure at the station outside the path of total eclipse.

ment of exposure, or, in the case under discussion, at the moment of maximum phase of obscuration, the direction of their relative motion corresponding to the vertical in the diagram. The space between the two arcs corresponding to the limbs of the sun and moon represents the remaining bright crescent. The larger circle must represent the apparent or augmented diameter of the moon. The chromospheric layer corresponding to the tip of an arc is represented by the dotted circle. The distance between the centers differs from the difference of radii by the distance between the limbs or width of the crescent.

Let the quantities involved be defined as follows:  $d$  equals the distance of the moon's center from the observing station;  $D$ , the distance of the moon's center from the earth's center;  $\rho$ , the distance of the observing station from the earth's center;  $z$ , the geocentric zenith distance of the moon;  $\pi$ , the moon's equatorial horizontal parallax;  $R_s$ , the sun's semi-diameter;  $R_m$ , the moon's apparent or augmented semi-diameter;  $R_{mg}$ , the moon's geocentric semi-diameter;  $\alpha$ , the angle at the moon's center subtending the half-arc of spectral line;  $\beta$ , the angle at the moon's center subtending the half-arc of the moon's limb within the crescent;  $\gamma$ , the angle at the sun's center subtending the half-arc of the sun's uncovered limb;  $h'$ , the central width of the crescent;  $h$ , the apparent height above the sun's surface of the emitting gas; and  $c$ , the distance between centers of sun and moon.

The quantities  $\rho$ ,  $\pi$ ,  $R_s$ ,  $R_{mg}$ , are taken from the American Ephemeris;  $D$  is given by  $\pi$ ; the zenith distance is computed from the apparent hour-angle corresponding to the time of the observation; and the angles are computed from the above-mentioned measures of the negative. Then  $d$ ,  $R_m$ ,  $h'$ ,  $h$ ,  $c$ , are computed from the following formulae:

$$d^2 = D^2 + \rho^2 - 2\rho D \cos z,$$

$$R_m = R_{mg} D/d,$$

$$h' = R_s(1 - \cos \gamma) - R_m(1 - \cos \beta),$$

$$h = \frac{R_m}{R_s}(R_m - R_s)(1 - \cos \alpha) - \left(1 - \frac{R_m}{R_s}(1 - \cos \alpha)\right)h',$$

$$c = R_m - R_s + h'.$$

The quantities in the first formula are expressed in terms of the earth's equatorial radius as unity. All the other quantities are expressed in seconds of arc. The formula for the height is derived from the triangle formed by the cusp and centers of sun and moon. The squares of the small quantities representing the height and width of the crescent are neglected in the equation here given. The final values for heights of the chromospheric gases are expressed in kilometers by multiplying the quantities  $h$  by the ratio of the sun's



diameter in kilometers to its diameter in seconds of arc. This factor is 712.2.

#### FURTHER RESULTS OF MEASURES AND COMPUTATIONS

The value of the augmented semi-diameter of the moon is found to be  $1003''.14$  while the sun's semi-diameter is  $976''.65$ . These give a difference of  $26''.49$  and a ratio of 1.027. From the expression for  $h'$  the central width of the crescent as derived from the plate is  $0''.84$ . A corresponding value of  $0''.60$  is derived from the value of magnitude of the eclipse 0.99969 which is computed from data of the American Ephemeris. The value derived from the plate may be too large if the exposure were not exactly at maximum phase and because the crescent was changing during the exposure. These values give 0.9 and 0.6 miles, respectively, as the distance of the observer from the cone of the shadow. That is, the edge of the shadow passed at a distance of about three-quarters of a mile (1.2 km) to the southward of the Observatory.

The interval before totality on the central line allowable for starting an exposure for the bright chromospheric lines without unduly darkening the plate may perhaps be judged from the present observation. The negative was slightly darkened. The rate of the moon's advancing edge is the difference of apparent diameters divided by the interval between second and third contacts. For New Haven this rate was  $0''.44$  per second of time. To cover the crescent of  $0''.6$  or  $0''.8$  would require approximately one and a half seconds. An observation on the central line with this apparatus could not have been safely begun more than two seconds before totality.

The circumstances attending the observation permit a determination of the difference of declination of the sun's and moon's centers. Since the prism was mounted with its refracting edge perpendicular to the hour-circle, the dispersion was in the direction of declination. If the crescent was perpendicular to the hour-circle at the moment of exposure, the centers of the sun and moon were on the same hour-circle. The negative shows that they were approximately so arranged, since the continuous band due to the crescent is nearly in the middle of the arcs and rings and parallel to the hour-circle. Since the distance between the centers is the difference of the radii *plus* the width of the crescent, the small quantity  $c$  is then

a very close measure of the difference of apparent declinations of the sun and moon at the time of the present observation. Its value is  $27''.33$ . The computation of the sun's and moon's apparent declinations from the data of the Nautical Almanac gives a difference of moon *minus* sun equal to  $-28''.18$ . This indicates a correction to the almanac value of the moon's declination of  $\Delta \delta = +0''.85$ . This may be compared with the  $+0''.87$  derived from Professor E. W. Brown's<sup>1</sup> correction to the moon's latitude  $\delta\beta = +0''.80$  which he derived from numerous observed times of second contact and duration of totality.

#### HYDROGEN ARCS

The Balmer series of hydrogen lines or arcs in the accompanying photograph show a significant decrease in length and intensity from  $H\alpha$  toward the violet. They could be enveloped by nearly straight lines converging to the axis of the arcs in the ultra-violet. Again the computed heights, as plotted in the accompanying diagram (Fig. 2), show a fairly regular decrement with decreasing wave-length and strongly indicate a relation between height and the series frequencies. A curve could be drawn among the points, but its significance would not be obvious. The lengths of spectrum arcs in a photograph of the chromospheric crescent are related mainly to the observable heights to which the radiating gases extend, but are affected by several factors: duration of exposure, transmission coefficients of the atmosphere and the optical parts of the apparatus, color sensitivity of the photographic emulsion, intensity of the source of radiation, and the effective area of source which is gradually narrowed by the moon's limb. In the case of a spectral series of lines originating from the same kind of atom other factors are involved. A decrease in intensity of successive members has been found in every source of the hydrogen lines thus far observed. It is mentioned in particular by Evershed<sup>2</sup> in his reports of the chromospheric spectrum of the eclipses of 1898 and 1900. The hydrogen lines are also observed to behave in the chromosphere like the enhanced lines which with increase of height increase in intensity relative to the Fraunhofer lines although they may decrease with the reduction of the solar

<sup>1</sup> *Astronomical Journal*, No. 866, 37, 18, 1926.

<sup>2</sup> *Philosophical Transactions of the Royal Society*, 197, 400, 1901; A, 201, 462, 1903.

atmospheric temperature and density. These factors render the gradients of the line-intensities dissimilar. If the intensities of the radiations of the series lines were uniform throughout the observed thickness of chromosphere, the relative heights derived from the observed lengths of the arcs would be due in the main to the relative intensities of the series lines. But in view of the many factors involved, the relative heights are due only in part to their relative intensities. No definite determination of intensities and their ratios has yet been

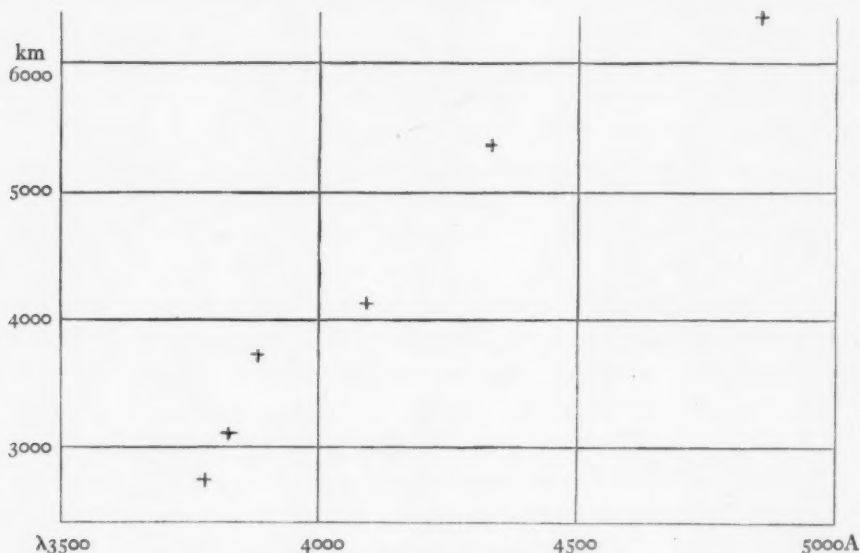


FIG. 2.—Heights for the hydrogen arcs

made. Many observers have made estimates which represent only grades in amount of photographic impression produced by the successive lines. Several of these are collected in Table II merely to show what there may be of relation among these results. The second column gives the hundreds of kilometers from Table I and their ratios for adjacent lines. In the fourth column are given general averages of Wright's numbers. The numbers in the last column are those implied by the ratios given by Wood for the relative intensity of successive lines in a laboratory source, the vacuum tube. There is obviously great variance in the systems of estimates of intensities, and these may cover considerable variation in the ratios of intensity

of successive members of series observed in various sources involving different conditions of excitation.

TABLE II

LINES	HEIGHTS	CHROMOSPHERE			NEBULAE Wt. §	VACUUM TUBE W
		D*	M †	A ‡		
H $\beta$ 4861.....	63	{ 100	100	200	52	112
H $\gamma$ 4340.....	53		80	200	47	48
H $\delta$ 4101.....	41		70	150	27	21
H $\epsilon$ 3970.....		30	60		15	9
H $\zeta$ (He) 3889.....	37	{ 20	60	100	17]	4
H $\eta$ 3835.....	31		55	50	8	2
H $\theta$ 3798.....	28		50	50	5	1

\* Dyson, *Philosophical Transactions of the Royal Society*, A, 206, 438, 1906.

† Mitchell, *Astrophysical Journal*, 38, 407, 1913.

‡ Anderson, *Publications of the United States Naval Observatory*, 10, B157, 1926.

§ Wright, *Publications of the Lick Observatory*, 13, 246, 1918.

|| Wood, *Proceedings of the Royal Society*, A, 97, 461, 1920.

## CONCLUSION

The quality of the negatives obtained in the observation here described hardly permits of measurement of intensities; but this could be made feasible by properly planning the observation. The plates exposed could be given the customary graded exposures required for photometric scale and the color curve or color ratios obtained for the emulsion. Thence could be derived the gradients of intensities of the chromospheric lines with respect to height, and the ratios of intensity in series lines at various levels in the chromosphere. Data on these points are needed in the problem of the physical condition of the chromosphere and its radiation.

The observation showed that there is available an interval of many seconds for exposures on the chromospheric crescent with apparatus located close to the edge of the eclipse shadow. If the location is just within the shadow, the limb of the moon at central phase will obscure the lower region of the chromosphere. At a point just outside, the observer is certain of securing the full lengths of the

spectral arcs from the crescent corresponding to the actual solar surface out as far as the intensity of the radiation is able to affect the photographic emulsion. It is desirable that the spectral arcs be perpendicular at their midpoints to the line of dispersion in the negative. For this purpose the mounting of the prism should permit of rotation, so that the prism's edge may be set parallel to the tangent at the cusp of the crescent. For exposure at central phase on a very short crescent the prism's edge may be set parallel to the length of this short crescent.

Acknowledgments are due to Professor Philip Fox, of Dearborn Observatory, Northwestern University, and to Professor C. H. Currier, of Ladd Observatory, Brown University, for their generous interest in this work.

LADD OBSERVATORY AND DEARBORN OBSERVATORY

April 1927



## ON THE SPECTRA OF DOUBLY AND TREBLY IONIZED TITANIUM ( $Ti$ III AND $Ti$ IV)<sup>1</sup>

By HENRY NORRIS RUSSELL<sup>2</sup> AND R. J. LANG

### ABSTRACT

The lines of trebly ionized titanium ( $Ti$  IV) are peculiar to the spectrum of the vacuum spark. Those of  $Ti$  III appear in the ordinary spark, but are much enhanced in the vacuum source.

31 lines of  $Ti$  IV and 90 lines of  $Ti$  III have been identified. All of the former and most of the latter are new. Tables of wave-lengths and intensities based on plates obtained at Mount Wilson and Edmonton are given. The wave-lengths range from 5492 to 423 Å. All the lines of  $Ti$  IV and all but four of  $Ti$  III have been classified.

The spectrum of  $Ti$  IV is very regular and consists entirely of doublets, arranged in series conforming to the Ritz formula. Twelve lines, of types ranging from S to H, have been identified and are tabulated. The 3D term is the lowest, and the ionization potential is 43.06 volts. The doublet separations are in excellent agreement with Landé's formula.

The spectrum of  $Ti$  III includes triplet and singlet terms and is closely analogous to that of Sc II. Nineteen terms, of types ranging from S to G, have been identified. The lowest term is of type <sup>3</sup>F, followed by <sup>1</sup>D, <sup>3</sup>P, and <sup>1</sup>G. The observed terms are in perfect agreement with Hund's theory, arising from the electron configurations (3d)<sup>3</sup>, 3d·4s, 3d·4p, 3d·4d, and 4s·4p. The estimated ionization potential is 27.6 volts, with an uncertainty not exceeding 1 volt. The term separations are again in general agreement with Landé's formula.

The spectrum of Sc III is also briefly discussed. One new term is added (<sup>5</sup>S). All the strong lines of the spectrum which have not been observed must lie in the visible region. Their predicted positions are given.

Comparisons are made between the series spectra, K I, Ca II, Sc III, and  $Ti$  IV, and also Ca I, Sc II, and  $Ti$  III. Moseley's law as extended to the optical region is fully verified—the differences in  $\sqrt{\nu/R}$  being practically constant for similar terms, from one spectrum to the next. The identifications of certain doubtful terms are thus confirmed.

The senior author of this paper has for some time been engaged in an analysis of the spectrum of titanium, with the aid of material furnished by his colleagues at the Mount Wilson Observatory. During the course of this work, it became evident that certain lines must belong to multiply ionized atoms, and a number of multiplets of  $Ti$  III were identified. A full analysis of these spectra, however, is not possible without observations in the extreme ultra-violet; and these have been furnished by the work of the junior author. The present communication is therefore based upon observations made at Mount Wilson by Mr. Anderson and Miss Carter, and at

<sup>1</sup> Contributions from the Mount Wilson Observatory, Carnegie Institution of Washington, No. 337.

<sup>2</sup> Research Associate of the Mount Wilson Observatory, Carnegie Institution of Washington.

the University of Alberta by Mr. Lang, while Mr. Russell is responsible for the analysis and discussion.

#### I. THE OBSERVATIONS

The first definite evidence of the existence of lines of titanium corresponding to higher stages of ionization than the first was found by Miss Carter, in the spectrum of the discharge of a large condenser, such as is used in "exploding" fine wires, between electrodes of metallic titanium *in vacuo*. The spectrum was photographed with a concave grating of 1-m radius, and extends from the green to  $\lambda$  2100. The ordinary spark and arc spectra were taken on the same film for comparison.

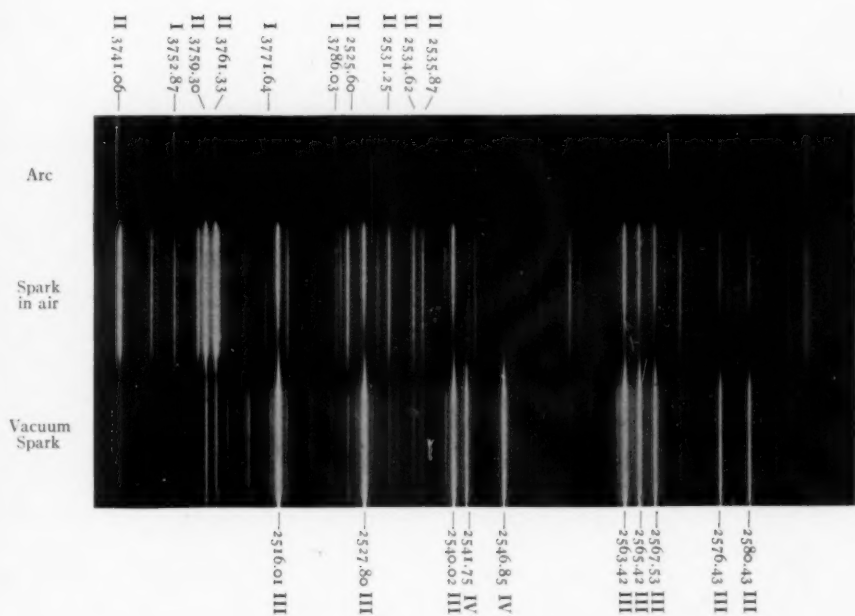
Most of the lines in the "hot-spark" spectrum agree with those of the ordinary spark (*Ti* II). The stronger arc lines show faintly, but are much weaker than in the ordinary spark. Certain lines, however, which appear in the latter spectrum—many of them strongly—are greatly enhanced in the hot-spark. These lines are completely absent from the arc spectrum, in which practically all the lines of *Ti* II are present; and they appear distinctly "polar" in the ordinary spark. All these properties indicate that these are lines of *Ti* III, which is confirmed by the fact that the strongest ones obviously come in three's, as should be expected in this spectrum. Besides these lines, however, the hot-spark shows others, some of them very strong, which are absent from the ordinary spark, and form conspicuous pairs. These must belong to *Ti* IV.

These lines are illustrated in Plate II, which shows the third order near  $\lambda$  2500 with the overlapping second order near  $\lambda$  3750. The principal lines of the metal in its four stages of ionization are marked on the margins. The differences in their behavior are very conspicuous and show how definitely the separation of the successive spectra can be made. Another photograph of the hot-spark spectrum taken by Dr. Anderson shows lines of *Ti* III and *Ti* IV down to  $\lambda$  1905.

This overlaps the region observed at Edmonton with the vacuum spectrograph. This instrument has been fully described elsewhere,<sup>1</sup> and it may suffice to say that the concave grating has a radius of

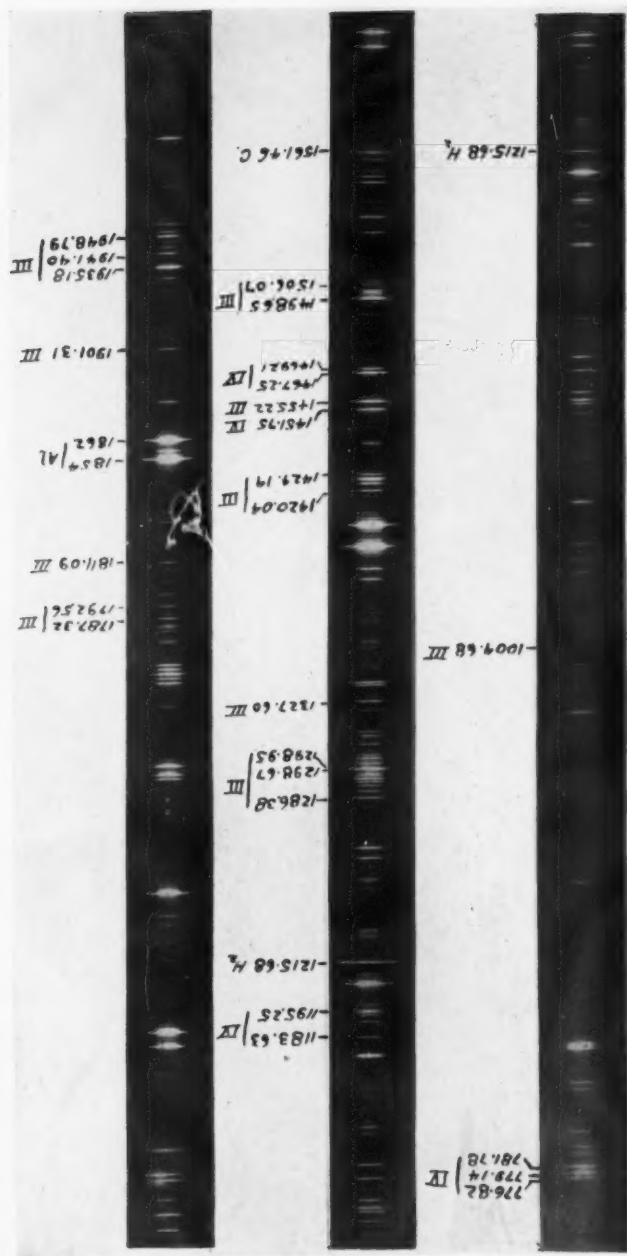
<sup>1</sup> *Journal of the Optical Society of America*, 12, 523, 1926.

## PLATE II



ARC, SPARK, AND VACUUM-SPARK SPECTRA OF TITANIUM  
Photographed at Pasadena by Miss Carter

### PLATE III



6 feet and 30,000 lines to the inch. The spectra obtained from the vacuum spark between electrodes of the best metallic titanium available showed the lines of silicon more strongly than those of the metal; but the former have been eliminated by comparison with the spectrum of the silicon spark, and other impurities were similarly eliminated. The remaining lines may be ascribed with some confidence to titanium. The strongest of them have been identified as belonging to *Ti* III or *Ti* IV; but the majority of the lines remain unclassified, and it is probable that most of these belong to *Ti* V, which, like *Ca* III, should be a very complex spectrum resembling that of argon. This spectrum is illustrated in Plate III.

The measures on the Edmonton spectrograms were made by Lang, using the standards recently determined by Smith and Lang.<sup>1</sup> From the agreement of the observed frequency differences with those derived from the analysis of the spectrum, it appears that the probable error of a measured wave-length is approximately  $\pm 0.02$  Å (see below). For the longer wave-lengths, Exner and Haschek's measures are available for many lines of *Ti* III, which appear in the ordinary spark. Some of these lines have been remeasured, and many new lines of *Ti* III and *Ti* IV have been measured for the first time, by Mr. Russell on positive enlargements of the Mount Wilson films. The probable error of the resulting wave-lengths appears to be about  $\pm 0.01$  Å.

## 2. THE SPECTRUM OF THE TREBLY IONIZED ATOM (*Ti* IV)

In discussing the results, it is well to begin with the simplest spectrum, which is that corresponding to the highest degree of ionization. From theoretical considerations, this should be of the "stripped-atom" type. All the terms should be doublets, and should be arranged in normal series, closely following the Ritz formula.

The lowest terms in this spectrum were discovered by Gibbs and White.<sup>2</sup> The base level is a  $^2D$  term, and the next a  $^1S$  term, both of which combine with a higher  $^3P$  term. The lines of the corresponding groups are conspicuous on the Edmonton photographs, as are

<sup>1</sup> *Physical Review*, **28**, 36, 1926.

<sup>2</sup> *Proceedings of the National Academy of Sciences*, **12**, 600, 1926.



also two other groups which evidently arise from combinations between the  $^2P$  term and higher-lying  $^2S$  and  $^2D$  terms. The strong pair shown on the Mount Wilson photograph in Plate II have proved to arise from a transition from the new  $^2D$  term to a  $^2F$  term, and other combinations revealed the existence of several higher levels. Three  $S$  terms, two  $P$ 's, four  $D$ 's, one  $F$ , one  $G$ , and two  $H$ 's were finally identified. Most of the new lines are in the region accessible with ordinary instruments; but the important pair,  $3D-4F$ , are in the extreme ultra-violet. Their computed positions, which can be very accurately found by the aid of other combinations, are at  $\lambda\lambda$  424.18, 423.50. Lines have been observed at  $\lambda$  424.28 and  $\lambda$  423.58, and these are evidently the pair in question, the systematic discordance of 0.09 Å being explicable by the lack of good standards in the region. This pair, and also the groups  $4P-5S$  and  $4P-4D$ , were independently identified by Mr. Stanley Smith, to whom we are indebted for the measures of these two lines.

The  $S$  terms are exactly represented by the Ritz formula

$$mS = 16R / \{m - 1.38265 - 2.55 \times 10^{-7}(mS)\}^2,$$

where  $m = 4, 5, 6$ . The term values referred to the limit of this series, with the Rydberg denominators,  $n^*$ , are given in Table I.

TABLE I  
SERIF'S TERMS FOR  $Ti$  IV

		$n^*$			$n^*$			$n^*$
4S <sub>1</sub> ....	268439.2	2.5568	3D <sub>1</sub> ....	348433.5	2.2442	4F <sub>4</sub> ....	112685.3	3.9463
				384.3	.00119		7.2	.00012
5S <sub>1</sub> ....	136422.0	3.5866	3D <sub>2</sub> ....	348817.8	2.2430	4F <sub>3</sub> ....	112692.5	3.9462
6S <sub>1</sub> ....	82982.0	4.5986	4D <sub>1</sub> ....	151937.3	3.3985	5G <sub>1</sub> ....	70316.7	4.9956
				85.7	.00095			
4P <sub>1</sub> ....	220086.0	2.8238	4D <sub>2</sub> ....	152023.0	3.3975	6H <sub>1</sub> ....	48805.3	5.9964
	818.4	.00534				7H <sub>1</sub> ....	25844.3	6.9970
4P <sub>2</sub> ....	220905.3	2.8185	5D <sub>1</sub> ....	89951.1	4.4179			
				39.5	.00007			
5P <sub>1</sub> ....	117904.4	3.8580	5D <sub>2</sub> ....	89990.6	4.4169			
	315.8	.00522						
5P <sub>2</sub> ....	118220.2	3.8528						

The spectrum is extremely regular in its structure. The differences of the denominator  $n^*$  for the successive pairs of terms of the same series are very nearly equal, as they should be, and the quantum defects for the "hydrogenic"  $G$  and  $H$  terms are very small. The terms  $6H$  and  $7H$  are each determined from only a single

TABLE II  
MULTIPLETS OF Ti IV

	$4P_2$	$4P_1$	$5P_2$	$5P_1$	$4F_4$	$4F_3$	$6H$	$7H$
$4S_1$ .....	{ (15) 48352.2 52.3	{ (10) 47534.1 33.9	(140535)	(140219)				
$5S_1$ .....	{ (5) 83604.5 64.9	{ (5) 84485.9 83.3	(8) 18517.6 17.6	(6) 18201.8 01.8				
$6S_1$ .....	{ (0) 137100.9 04.9	{ (137023)	(11) 34922.2 22.4	(on) 35238.4 38.2				
$3D_3$ .....	{ (20) 128346.6 46.6	{ (20) 127913.3 12.3	(230527)		(4) 235604 748	(235741)		
$3D_2$ .....	{ (10) 128730.0 30.9	{ (20) 127913.3 12.3	(230912)	(230597)		(3) 236083 125		
$4D_3$ .....	{ (30) 68150.0 49.6	{ (30) 68882.3 82.3	(5) 34032.4 32.9		(12) 39252.4 52.0	(3) 39245.5 45.1		
$4D_2$ .....	{ (15) 68003.7 63.9	{ (30) 68882.3 82.3	(1) 34118.1 18.6	(4) 33802.5 02.6		(8) 39331.1 30.5		
$5D_1$ .....	{ (130155)	{ (130096)	(4) 27952.8 53.3		(2) 22734.5 34.2	(22741.4)		
$5D_2$ .....	{ (130096)	{ (130015)	(27913.8)	(3) 28220.1 29.6		(2) 22702.6 01.9		
$5G$ .....					{ (5) 42368.7 68.7	(5) 42375.9 75.9	(3) 21511.4 11.4	(0) 34472.4 72.4

line, but their excellent agreement with the values which are to be anticipated is sufficient evidence of their reality.

All the series are nearly Ritzian. The expression  $0.4443 - 3.00 \times 10^{-7} (mD)$  has the values 0.3398, 0.3987, 0.4173, for the three D terms, so that the limit found from the last two, ignoring the first

TABLE III  
IDENTIFIED LINES OF  $Ti$  IV

$\lambda$ I.A.	Int.	$\nu$	Designation
Air			
5492.43.....	(6)	18201.8	5S <sub>1</sub> -5P <sub>1</sub>
5398.82.....	(8)	18517.6	5S <sub>1</sub> -5P <sub>2</sub>
4647.40.....	(3)	21511.4	5G-6H
4403.54.....	(2)	22702.6	4F <sub>3</sub> -5D <sub>2</sub>
4397.37.....	(2)	22734.5	4F <sub>4</sub> -5D <sub>3</sub>
3576.44.....	(4)	27952.8	5P <sub>2</sub> -5D <sub>3</sub>
3541.44.....	(3)	28229.1	5P <sub>1</sub> -5D <sub>2</sub>
2957.50.....	(4)	33802.5	4D <sub>2</sub> -5P <sub>1</sub>
2937.52.....	(5)	34032.4	4D <sub>3</sub> -5P <sub>2</sub>
2930.14.....	(1)	34118.1	4D <sub>2</sub> -5P <sub>2</sub>
2900.02.....	(0)	34472.4	5G-7H
2862.67.....	(1n)	34922.2	5P <sub>2</sub> -6S <sub>1</sub>
2836.98.....	(on)	35238.4	5P <sub>1</sub> -6S <sub>1</sub>
2547.30.....	(3)	39245.5	4D <sub>3</sub> -4F <sub>3</sub>
2546.85.....	(12)	39252.4	4D <sub>3</sub> -4F <sub>4</sub>
2541.75.....	(8)	39331.1	4D <sub>2</sub> -4F <sub>3</sub>
2359.51.....	(5)	42368.7	4F <sub>4</sub> -5G
2359.11.....	(5)	42375.9	4F <sub>3</sub> -5G
Vacuum			
2103.75.....	(10)	47534.1	4S <sub>1</sub> -4P <sub>1</sub>
2068.16.....	(15)	48352.2	4S <sub>1</sub> -4P <sub>2</sub>
1469.21.....	(15)	68063.7	4P <sub>2</sub> -4D <sub>2</sub>
1467.25.....	(30)	68150.0	4P <sub>2</sub> -4D <sub>1</sub>
1451.75.....	(30)	68882.3	4P <sub>1</sub> -4D <sub>2</sub>
1195.25.....	(5)	83664.5	4P <sub>2</sub> -5S <sub>1</sub>
1183.63.....	(5)	84485.9	4P <sub>1</sub> -5S <sub>1</sub>
781.78.....	(20)	127913.3	3D <sub>2</sub> -4P <sub>1</sub>
779.14.....	(20)	128346.6	3D <sub>3</sub> -4P <sub>2</sub>
776.82.....	(10)	128730.0	3D <sub>2</sub> -4P <sub>2</sub>
729.39.....	(0)	137100.9	4P <sub>2</sub> -6S <sub>1</sub>
424.28.....	(3)	235694	3D <sub>3</sub> -4F <sub>4</sub>
423.58.....	(4)	236083	3D <sub>3</sub> -4F <sub>3</sub>

term, would agree very closely with that given by the S series. The normal state, 3D, is at a considerably lower level than the formula derived from the rest of the series would indicate, as happens often in other similar series. It is evident that all the series have the same limit, which should be determined with a probable uncertainty of only about 20 frequency units. The normal state of the trebly

ionized atom corresponds to the  $3^2D_2$  term, and the ionization potential is 43.06 volts.

The observed combinations between these terms are listed in Table II, which gives the wave-numbers alone, as the wave-lengths are found in Table III. The intensity of each line is given in parentheses above the observed wave-number, while the last three figures of the wave-number, computed from the data of Table I, are given below it. The computed wave-numbers of a few lines which have not been observed are given in parentheses.

It is noteworthy that no long series have been found. Only the leading member of the series which corresponds to transitions between a given level and the higher levels is strong; the next, if observable, is weak. This is a well-known characteristic of the vacuum spark.

A complete list of the lines which have been identified by their series relations as belonging to *Ti* iv is given in Table III. Certain other lines which appear in the hot-spark and may belong to this spectrum, but cannot be definitely identified, are listed in Table X.

### 3. A NOTE ON *Sc* III

The ultimate lines of *Sc* III have been detected by Gibbs and White,<sup>1</sup> and additional lines have been found by Stanley Smith<sup>2</sup> on plates taken by one of us. His identification of the group near  $\lambda$  2000 as 4P-4D rather than 4P-5S appears to be correct. The term values which he gives are derived on the assumption that  $4F=62,570$ , corresponding to the Rydberg denominator 3.9720. The corresponding denominators for *K* I, *Ca* II, and *Ti* IV are 3.9930, 3.9801, and 3.9463. Smith's value was obtained by extrapolation from the first two of these; now that the last is known, interpolation gives the presumably more accurate value 3.9640, whence  $4F=62,822$ , so that all his term values may be increased by 250, a hardly significant correction. The resulting term values and Rydberg denominators are entered in Table IV, and also the values for other terms not yet observed, but predicted as follows. The denominators  $n^*$  for *K* I, *Ca* II, and *Ti* IV are accurately known,

<sup>1</sup> *Proceedings of National Academy of Sciences*, 12, 598, 1926.

<sup>2</sup> *Ibid.*, 13, 66, 1927.

and hence the differences of the fractional part of their values for the successive terms of the same series (which depend upon the "Ritz correction"). These differences are small and run smoothly so that they can be interpolated for *Sc* III with considerable confidence, as shown below where the estimated values are in parentheses.

	<i>K</i> I	<i>Ca</i> II	<i>Sc</i> III	<i>Ti</i> IV
5S - 4S.....	+0.0309	+0.0322	+0.0304	+0.0204
6S - 5S.....	.0090	.0126	(.013)	.0120
5P <sub>2</sub> - 4P <sub>2</sub> .....	.0313	.0362	(.037)	.0342
6P <sub>2</sub> - 5P <sub>2</sub> .....	+ .0095	.0126	(.014)	.....
4D <sub>3</sub> - 3D <sub>3</sub> .....	- .0570	.0461	.1362	.1543
5D <sub>3</sub> - 4D <sub>3</sub> .....	.0280	.0071	(.022)	+0.0194
6D <sub>3</sub> - 5D <sub>3</sub> .....	.0130	+ .0031	(+ .011)	.....
5F <sub>4</sub> - 4F <sub>4</sub> .....	-0.0028	-0.0035	(-0.005)	.....

In this way it was predicted that the value of  $n^*$  for 5S should be  $3.420 \pm 0.002$  and the term itself  $84,900 \pm 100$ . This leads to the identification of  $4P_2 - 5S$  as  $\lambda 1912.48$  (intensity 2) for which  $n = 52,288$ , making  $5S = 84,829$ .

There is also a line of intensity 2 on the scandium plates at  $\lambda 1895.33$  ( $n = 52761.3$ ), which appears with equal intensity in the spectrum of silicon, and faintly in that of titanium. It is in exactly the right place for  $4P_1 - 5S$ , and is probably a blend of a scandium line with some impurity.

We then have the results shown in Table IV.

TABLE IV  
OBSERVED AND PREDICTED TERMS OF *Sc* III

	Observed	$n^*$		Predicted	$n^*$
4S.....	174156.3	2.3808	6S.....	50440	4.424
5S.....	84829.2	3.4112	5P <sub>2</sub> .....	71330	3.720
4P <sub>2</sub> .....	137117.1	2.6831	5P <sub>1</sub> .....	71510	3.715
	473.7	.0046	5D <sub>3</sub> .....	51410	4.382
4P <sub>1</sub> .....	137590.8	2.6785	5D <sub>2</sub> .....	51430	4.381+
3D <sub>3</sub> .....	199495.5	2.2244	5F.....	40140	4.959
	197.5	.00110	5G.....	39560	4.995
3D <sub>2</sub> .....	199693.0	2.2233			
4D <sub>3</sub> .....	87393.8	3.3601			
	45.0	.00086			
4D <sub>2</sub> .....	87438.8	3.3592			
4F.....	62822.0	3.9640			



The combinations of the predicted terms with the low terms give lines in the far ultra-violet, which, from the well-known properties of the vacuum spark, might be expected to be very faint. They have not been found. Judged by the analogy of *Ti* IV, the lines in the visible region should be much stronger. Those which might be expected to appear are, in the order of their probable intensity,

5S-5P.....	7406, 7506
4D-5P.....	6223, 6276, 6206
4F-5G.....	4298 (close double)
5P-5D.....	5018, 4978, 5023
4F-5D.....	8762, 8777

It is noteworthy that all these lines lie in the visible region, and about half of them in the red.

#### 4. COMPARISON OF *K* I, *Ca* II, *Sc* III, *Ti* IV, ETC.

It is well known that the term values in atomic systems which contain the same number of electrons exhibit marked regularities.

The values of  $\sqrt{\nu/R}$  (where  $R$  is the Rydberg constant, and  $\nu$  any given spectroscopic term, referred to the limit of the series to which it belongs) form an arithmetical progression for successive atoms in order of atomic number.

The constant difference in this progression is nearly the same for all terms involving an electron of the same total quantum number; whence it follows that the wave-numbers of lines corresponding to transitions of an electron between two orbits of the same total quantum number will themselves be in arithmetical progression with increasing atomic number (which is the irregular doublet law).

A thorough test of these relations can be made by comparison of terms from successive spectra *K* I<sup>1</sup>, *Ca* II<sup>2</sup>, *Sc* III, and *Ti* IV. The values of  $\sqrt{\nu/R}$  for such terms as have been identified in *Ti* IV are given in Table V with the differences  $\Delta$  between each spectrum and the next.

The terms are arranged in order of their total quantum numbers,

<sup>1</sup> Fowler, *Report on Series in Line Spectra* (London, 1922).

<sup>2</sup> Saunders and Russell, *Astrophysical Journal*, 62, 1, 1925.

according to Bohr's theory of atomic structure, and the means of the two components of the double terms are taken.

Certain values of  $\nu$  which have not been observed, but can be rather accurately estimated (including those in *Sc III*, discussed above), are given in parentheses in the table, as are the differences involving them. The differences in  $\sqrt{\nu/R}$  are not constant, but run very smoothly. For *V v*, for which the data given by Gibbs

TABLE V  
VALUES OF  $\sqrt{\nu/R}$

Term	K I	Diff.	Ca II	Diff.	Sc III	Diff.	Ti IV	Diff.	V v
3D.....	0.350	0.535	0.865	0.484	1.349	0.434	1.783	0.407	2.190
4S.....	.565	.369	.934	.326	1.260	.305	1.565	.292	1.857
4P.....	.448	.353	.801	.310	1.120	.298	1.418	(0.288)	1.706
4D.....	.263	.334	.597	.296	0.893	.284	1.177	.....	.....
4F.....	.250	.252	.502	.255	.757	.257	1.014	.....	.....
5S.....	.357	.273	.630	.250	.880	.235	1.115	.....	.....
5P.....	.306	.260	.566	(.242)	(.808)	(.229)	1.037	.....	.....
5D.....	.210	.248	.458	.227	(.685)	(.220)	0.905	.....	.....
5F.....	.200	.202	.402	.....	.....	.....	.....	.....	.....
5G.....	.200	.200	(.400)	(.200)	(.600)	(.201)	.801	.....	.....
6S.....	.263	.204	.467	(0.210)	(0.677)	(0.193)	.870	.....	.....
6P.....	.234	.206	.440	.....	.....	.....	.....	.....	.....
6D.....	.174	.198	.372	.....	.....	.....	.....	.....	.....
6F.....	.167	0.167	.334	.....	.....	.....	.....	.....	.....
6G.....	.....	.....	0.333	.....	.....	.....	.....	.....	.....
6H.....	0.166	.....	.....	.....	.....	.....	0.667	.....	.....

and White suffice only to determine the differences of the terms 3D, 4S, 4P, the mean value of the last-named term has been derived on the assumption that the difference of  $\sqrt{\nu/R}$  was the same as the mean value for the two preceding difference columns. This gives  $4P_2 = 318,567$ ,  $4P_1 = 319,833$ ,  $4S = 378,113$ ,  $4D_3 = 525,613$ ,  $5D_2 = 526,250$ . The differences of  $\sqrt{\nu/R}$  for 3D and 4S can then be determined, and fit smoothly into the scheme. The identification of further terms in this spectrum is much to be desired.

The pairs 4S-4P have been identified by Gibbs and White<sup>1</sup> for *Cr VI* and *Mn VII*. On taking the mean of the two lines (as above) and estimating the values of  $\sqrt{\nu/R}$  for 4P as 1.996 and 2.286, by adding the difference 0.290 twice more, the resulting values for 4S are found to be 2.149 and 2.442, giving two new horizontal differences of 292 and 293, which fit perfectly into the scheme. This means, however, only that the irregular doublet law is closely followed, as Gibbs and White have already pointed out.

<sup>1</sup> *Proceedings of the National Academy of Sciences*, 12, 676, 1926.

For the separation  $\Delta\nu$  of the components of a doublet term, two formulae have been given. The first is the "regular doublet law," extended to the optical region by Millikan and Bowen.<sup>1</sup> According to this  $\Delta\nu = K(Z-s)^4$ , where  $K$  has the value 0.0456 for 4P terms, 0.0234 for 5P, 0.036 for 3D, 0.0152 for 4D, and 0.0076 for 4F, and  $s$  is a screening constant, which may be expected to be roughly constant, decreasing slowly along any given series of "stripped atoms."

Gibbs and White have given the values of  $s$  for the 4P terms, and those computed from the formulae for other terms are added here:

	K I	Ca II	Sc III	Ti IV	V V	Cr VI	Mn VII
4P.....	13.04	11.64	10.91	10.43	10.09	9.85	9.75
5P.....	13.68	12.40	(11.62)	11.22	.....	.....	.....
3D.....	16.04	13.59	12.40	11.84	11.48	.....	.....
4D.....	.....	15.13	13.61	13.32	.....	.....	.....
4F.....	.....	.....	.....	12.13	.....	.....	.....

The screening numbers  $s$  are of the same order of magnitude, but the differences among them are considerable, and correspond to very much greater proportional differences in the values of  $\Delta\nu$ .

The second law of separation is that suggested by Landé, and since then found to be deducible from the theory of the spinning electron. It may be written

$$\Delta\nu = \frac{Ra^2Z_a^2Z_i^2}{K(K+1)n^{*3}},$$

where  $R$  and  $a$  have their usual meanings,  $K=1$  for P terms, 2 for D terms, etc.,  $n^*$  is the Rydberg denominator,  $Z_a$  is the effective nuclear charge for the outer part of the electron orbit, and is 1 for the neutral atom, 2 for the singly ionized atom, etc., and  $Z_i$  is the effective charge for the inner part of the orbit (which may be written in the form  $Z-s$ , where  $s$  is a new screening constant). The corresponding differences in the Rydberg denominator are given by the much simpler formula

$$\Delta n = \frac{a^2Z_i^2}{2K(K+1)},$$

( $a^2=5.31 \times 10^{-5}$ ). This difference should therefore be constant.

<sup>1</sup> *Physical Review*, 24, 209-233, 1924.

The values of  $\Delta n$  are actually nearly constant for each series in  $K\ I$ ,  $Ca\ II$ , and  $Ti\ IV$ , so far as they have been observed. For the other stripped atoms of this series only the values for the leading terms are known, and therefore the values for these terms alone are tabulated below, with the resulting values of  $s$ .

In determining  $\Delta n$  for the last three spectra, the values of  $\sqrt{\nu/R}$  derived above have been used.

TABLE VI  
DOUBLET SEPARATIONS

	$K\ I$	$Ca\ II$	$Sc\ III$	$Ti\ IV$	$V\ V$	$Cr\ VI$	$Mn\ VII$
4P:							
$\Delta\nu$ .....	57.5	222.8	473.8	818.4	1265	1822	2465
$10^5 \Delta n$ .....	295	392	486	524	560	592	618
$Z_i$ .....	14.9	17.2	19.1	19.9	20.6	21.1	21.6
$s$ .....	4.1	2.8	1.9	2.1	2.4	2.9	3.4
3D:							
$\Delta\nu$ .....	2.74	60.8	197	384.5	637	.....	.....
$10^5 \Delta n$ .....	29	86	113	119	135	.....	.....
$Z_i$ .....	8.1	11.7	16.0	16.4	17.4	.....	.....
$s$ .....	10.9	8.3	5.0	5.6	5.6	.....	.....
4F:							
$\Delta\nu$ .....	.....	.....	.....	7.3	.....	.....	.....
$10^5 \Delta n$ .....	.....	.....	.....	12	.....	.....	.....
$Z_i$ .....	.....	.....	.....	7.4	.....	.....	.....
$s$ .....	.....	.....	.....	14.6	.....	.....	.....

For the P terms the values of  $s$  are remarkably steady and run very smoothly. In this case, the tabulated numbers are the differences of two rather large quantities, and the inequality of their values corresponds to far less percentage difference in the doublet separations than in the case of the other formula. When it is further considered that Landé has shown<sup>1</sup> that his formula represents all the doublets in the arc and spark spectra of alkali-like structure from  $Li$  to  $Ra^+$ , with values of  $s$  ranging only from 2 to about 8, it is evident that it gives really a remarkable approximation to the truth.

Why it is better than the "relativity doublet" formula becomes clear when it is considered that the latter is derived on the assumption that the electron moves throughout its orbit in a Coulomb field of intensity corresponding to the nuclear charge  $Z - s$ , while Landé's

<sup>1</sup> *Zeitschrift für Physik*, 25, 46; 1924.

formula is based on the assumption of an effective charge of different amounts  $Z_i$  and  $Z_a$  in the inner and outer parts of the orbit. As several simplifying assumptions were made in deriving it, it is not to be expected that  $s$  should come out exactly the same in all cases.

For the D terms the values of  $s$  are greater, which might be expected, as the d orbits do not penetrate so deeply into the atomic structure. The screening appears to be exceptionally great in the case of potassium, giving a very narrow doublet. This may well be connected with the small quantum defect and the nearly hydrogenic character of the 3d orbit in this atom. The screening for the 4F term, in the single case where this is known, is still greater.

#### 5. THE SPECTRUM OF DOUBLY IONIZED TITANIUM (*Ti* III)

The conspicuous groups near  $\lambda$  2500, two of which are shown in Plate II, are evidently due to *Ti* III. The stronger lines are given by Exner and Haschek; a number of weaker ones were added from the Mount Wilson plates. With the aid of these, multiplets were found corresponding to transitions from a  $^3D$  term to a triad of terms  $^3P$ ,  $^3D'$ ,  $^3F$ . The strong isolated line at  $\lambda$  2985 was identified as a  $^1D - ^1D'$  combination, and a few faint intersystem combinations were located.

On theoretical grounds, there was reason to anticipate the existence of  $^3P'$  and  $^3F'$  terms, lower than the  $^3D$ , and combining with the  $P$ ,  $D'$ ,  $F$  triad. The corresponding multiplets were easily found in the list of lines measured at Edmonton. Two of the three strongest lines of the group  $^3F' - ^3D'$  are too close to resolve even in the second order, and the third falls just upon the strongest line of a multiplet of silicon (which shows strongly as an impurity in the titanium). Comparisons with the spectrum of pure silicon, however, show that the line in question is considerably strengthened when titanium is present.

This completes the list of easily recognizable multiplets; but further progress was made by comparison with the very similar spectrum of *Sc* II,<sup>1</sup> aided by the values of  $\sqrt{\nu/R}$  for this spectrum and for *Ca* I. In this way a considerable group of lines lying between  $\lambda$  1700 and  $\lambda$  1960 was assorted into multiplets corresponding to

<sup>1</sup> Russell and Meggers, *Scientific Papers of the Bureau of Standards* (in press).

transitions from the  $^3P$ ,  $^3D'$ ,  $^3F$  triad, to a higher-lying "pentad" of terms  $^3S$ ,  $^3P'$ ,  $^3D$ ,  $^3F'$ ,  $^3G$ , while a group of faint lines near  $\lambda$  1000 was identified as a  $^3D-^3P$  multiplet like that near  $\lambda$  2500 in *Sc* II. In addition to these, a few lines which could not be identified by the combination principle have been classified with the aid of the values of  $\sqrt{\nu/R}$ . In most cases this identification is practically certain. In a few, where it is more doubtful, the corresponding terms are marked with a colon in the list. The arguments in favor of these identifications are given in section 7.

Table VII gives a list of all the terms which have thus been identified, and shows with what other terms they have been observed to combine. The term values are counted *upward* from the lowest-known level,  $^3F'_{2,1}$ , which is doubtless the lowest for the atom in this state of ionization.

The multiplets resulting from the combinations of these terms are given in Table VIII, which is arranged like Table II. In some cases a line which is believed to be a blend is listed in more than one place.

The multiplets arising from combinations between the low terms and the middle triad are strong, and all the predicted lines of importance are observed, except for some blends too close to be resolvable. The groups arising from transitions from the middle triad to the higher levels are faint and incomplete—so much so, indeed, that, if nothing but the data of Table VIII were available, the reality of the term  $b^3D$  would be very doubtful. Strong confirmation of the arrangement given above is found, however, by comparison with an exactly similar group of multiplets in *Sc* II, which are much stronger, and substantially complete, so that their interpretation cannot be doubted.

The energy levels of the leading components of the five terms involved, relative to  $^3G_5$  as origin, and the separations of the components of the terms, are as follows:

Term .....	$^3G$	$^3F'$	$^3D$	$^3P'$	$^3S$
Level <i>Sc</i> II .....	0	3072	-454	4250	616
Level <i>Ti</i> III .....	0	3901	547	6251	3371
Separation <i>Sc</i> II ....	108.8, 81.3	83.3, 70.5	72.4, 54.4	59.1, 31.2	....
Separation <i>Ti</i> III ....	216.7, 159.7	164.0, 143.5	145.6, ....	121.7, 58.9	....



The relative levels of the five terms oscillate in just the same way, while the component separations are in all cases very nearly twice as great for *Ti* III as for *Sc* II. The similarity of the two sets of

TABLE VII  
TERMS OF *Ti* III

Desig.	Level	Combinations	Desig.	Level	Combinations
$a^3F'_2$ .....	0.0	$a^3D', a^3F$	$a^3P_0$ ....	80943.95	$\{a^3S, a^3P', b^3P'$
	183.7			-5.93	$a^3D$
$a^3F'_3$ .....	183.7		$a^3P_1$ ....	80938.02	$b^3D$
	238.2			85.58	
$a^3F'_4$ .....	421.9		$a^3P_2$ ....	81023.60	
$a^1D_2$ .....	8472.6	$\{a^1P, a^1D', a^1F$	$a^1F_3$ ....	83116.58	$a^1D$
		$a^3D'$			
$a^3P_0$ .....	10536.4	$a^3P, a^3D', a^3F$	$a^1P_1$ ....	83795.70	$a^1D$
	67.1				
$a^3P_1$ .....	10603.5		$a^3G_3$ ....	129096.3	$a^3F$
	117.6			159.7	
$a^3P_2$ .....	10721.1		$a^3G_4$ ....	129256.0	
$a^1S_0$ .....	14052.7?	$a^1P, a^3P?$		216.6	
			$a^3G_5$ ....	129472.6	
$a^1G_4$ .....	14398.5	$a^1F$	$b^3D_1$ ....	.....	$a^3D'$
$a^3D_1$ .....	38063.50	$a^3P, b^3P, a^3D'$	$b^3D_2$ ....	129873.9	
	134.48			145.6	
$a^3D_2$ .....	38197.98	$a^3F$	$b^3D_3$ ....	130019.5	
	227.21				
$a^3D_3$ .....	38425.19	$a^1D'$	$a^3S_2$ ....	132854.6	$a^3P$
$b^3D$ .....	41703.65	$\{a^1P, a^1D', a^1F$	$b^3F'_2$ ....	133067.2	$a^3D', a^3F$
		$a^3P, a^3D', a^3F$		142.5	
$a^1D'$ .....	75197.43	$\{a^1D, b^3D$	$b^3F'_3$ ....	133209.7	
		$a^3D$		164.0	
$a^3D'_1$ .....	76999.70	$\{a^3P', b^3P', a^3D,$	$b^3F'_4$ ....	133373.7	
	166.95	$b^3D, a^3F', b^3F'$			
$a^3D'_2$ .....	77166.65	$a^1D, b^3D$	$b^3P_0$ ....	135543.8	$a^3P, a^3D'$
	257.55			58.6	
$a^3D'_3$ .....	77424.20		$b^3P'_1$ ....	135602.4	
				121.7	
$a^3F_2$ .....	77421.48	$a^3P', a^3D, a^3F'$	$b^3P'_2$ ....	135724.1	
	324.70				
$a^3F_3$ .....	77746.18	$b^3F', a^3G$	$b^3P_0$ ....	137262	$a^3D$
	412.53			228	
$a^3F_4$ .....	78158.71	$b^3D$	$b^3P_1$ ....	137490	
				481	
			$b^3P_2$ ....	137971	

terms would therefore appear to be beyond question. The faint multiplet  $a^3D - b^3P$  was found by means of the differences in  $\sqrt{\nu/R}$  from corresponding terms in *Sc* II and *Ca* I.

TABLE VIII  
MULTIPLETS OF  $T_2$  III

	$a^1F_4$	$a^1F_3$	$a^1F_2$	$a^1D_3$	$a^1D_2$	$a^1D_1$	$a^1P_3$	$a^1P_1$	$a^1P_0$
$a^1F'_4$	$\begin{Bmatrix} (40) \\ 77737.5 \\ 37.0 \end{Bmatrix}$	$\begin{Bmatrix} (30) \\ 77323.9 \\ 24.5 \end{Bmatrix}$	.....	$\begin{Bmatrix} (50) \\ 77001.9 \\ 02.5 \end{Bmatrix}$	.....	.....	.....	.....	.....
$a^1F'_3$	$\begin{Bmatrix} (3) \\ 77973.3 \\ 75.0 \end{Bmatrix}$	$\begin{Bmatrix} (30) \\ 77560.2 \\ 62.5 \end{Bmatrix}$	$\begin{Bmatrix} (50) \\ 77239.8 \\ 37.8 \end{Bmatrix}$	$\begin{Bmatrix} (50) \\ 77239.8 \\ 40.5 \end{Bmatrix}$	$\begin{Bmatrix} (40) \\ 76985.3 \\ 83.0 \end{Bmatrix}$	.....	.....	.....	.....
$a^1F'_2$	$\begin{Bmatrix} \dots\dots\dots \\ (77746.2) \\ \dots\dots\dots \end{Bmatrix}$	$\begin{Bmatrix} \dots\dots\dots \\ (77746.2) \\ \dots\dots\dots \end{Bmatrix}$	$\begin{Bmatrix} (20) \\ 77420.0 \\ 21.5 \end{Bmatrix}$	.....	$\begin{Bmatrix} (30) \\ 77168.3 \\ 66.7 \end{Bmatrix}$	$\begin{Bmatrix} (50) \\ 77001.9 \\ 999.4 \end{Bmatrix}$	.....	.....	.....
$a^1D_2$	.....	.....	.....	$\begin{Bmatrix} (2) \\ 68951.8 \\ 51.6 \end{Bmatrix}$	.....	.....	.....	.....	.....
$a^1P'_3$	.....	$\begin{Bmatrix} (5) \\ 67025.0 \\ 25.1 \end{Bmatrix}$	.....	$\begin{Bmatrix} (20) \\ 66703.5 \\ 03.1 \end{Bmatrix}$	$\begin{Bmatrix} 5d \\ 66449.2 \\ 45.6 \end{Bmatrix}$	.....	$\begin{Bmatrix} (25) \\ 70303.2 \\ 02.5 \end{Bmatrix}$	$\begin{Bmatrix} (20) \\ 70216.8 \\ 16.9 \end{Bmatrix}$	.....
$a^1P'_1$	.....	.....	$\begin{Bmatrix} (1) \\ 66819.0 \\ 18.0 \end{Bmatrix}$	.....	$\begin{Bmatrix} (10) \\ 66561.9 \\ 63.2 \end{Bmatrix}$	$\begin{Bmatrix} (10) \\ 66398.0 \\ 96.2 \end{Bmatrix}$	$\begin{Bmatrix} (15) \\ 70420.5 \\ 20.1 \end{Bmatrix}$	$\begin{Bmatrix} (20) \\ 70338.8 \\ 34.9 \end{Bmatrix}$	$\begin{Bmatrix} (20) \\ 70338.8 \\ 40.4 \end{Bmatrix}$
$a^1P'_0$	.....	.....	.....	.....	.....	$\begin{Bmatrix} (10) \\ 66463.3 \\ 63.3 \end{Bmatrix}$	.....	$\begin{Bmatrix} (15) \\ 70401.7 \\ 01.6 \end{Bmatrix}$	.....
$a^1D_3$	$\begin{Bmatrix} (20) \\ 39733.52 \\ 33.52 \end{Bmatrix}$	$\begin{Bmatrix} (1) \\ 39320.95 \\ 20.99 \end{Bmatrix}$	.....	$\begin{Bmatrix} (15) \\ 38998.73 \\ 99.61 \end{Bmatrix}$	$\begin{Bmatrix} (5) \\ 38741.64 \\ 41.66 \end{Bmatrix}$	.....	$\begin{Bmatrix} (6) \\ 42598.52 \\ 98.41 \end{Bmatrix}$	.....	.....
$a^1D_2$	.....	$\begin{Bmatrix} (15) \\ 39548.20 \\ 8.20 \end{Bmatrix}$	$\begin{Bmatrix} (1) \\ 39224.08 \\ 3.50 \end{Bmatrix}$	$\begin{Bmatrix} (1) \\ 39226.23 \\ 26.22 \end{Bmatrix}$	$\begin{Bmatrix} (8) \\ 38968.31 \\ 8.67 \end{Bmatrix}$	$\begin{Bmatrix} (5) \\ 38801.79 \\ 1.72 \end{Bmatrix}$	$\begin{Bmatrix} (3) \\ 42825.71 \\ 25.62 \end{Bmatrix}$	$\begin{Bmatrix} (5) \\ 42740.02 \\ 40.04 \end{Bmatrix}$	.....
$a^1D_1$	.....	.....	$\begin{Bmatrix} (15) \\ 39357.96 \\ 7.98 \end{Bmatrix}$	.....	$\begin{Bmatrix} (1) \\ 39103.03 \\ 03.15 \end{Bmatrix}$	$\begin{Bmatrix} (8) \\ 38936.28 \\ 36.20 \end{Bmatrix}$	$\begin{Bmatrix} (1) \\ 42959.85 \\ 60.10 \end{Bmatrix}$	$\begin{Bmatrix} (3) \\ 42874.55 \\ 74.52 \end{Bmatrix}$	$\begin{Bmatrix} (3) \\ 42880.45 \\ 80.45 \end{Bmatrix}$

TABLE VIII—Continued

	aF <sub>4</sub>	aF <sub>3</sub>	aF <sub>2</sub>	aD <sub>3</sub>	aD <sub>2</sub>	aD <sub>1</sub>	aP <sub>2</sub>	aP <sub>1</sub>	aP <sub>0</sub>
b <sup>2</sup> D <sub>2</sub> .....		(1) 36041.90 42.53	(1) 35717.65 17.83	(0) 35719.97 20.65	(1) 35402.90 63.00			(0) 39234.35 34.37	
a <sup>3</sup> G <sub>5</sub> .....	(5) 51313.9 13.9								
a <sup>3</sup> G <sub>4</sub> .....	(1) 51098.1 97.3	(4) 51509.2 09.8							
a <sup>3</sup> G <sub>3</sub> .....		(3) 51074.8 74.8							
b <sup>2</sup> F' <sub>4</sub> .....	(2) 55215.5 15.0	(1) 55627.0 27.5		(2) 55949.7 49.5					
b <sup>2</sup> F' <sub>3</sub> .....		(55051.0) (55463.5) (55788.2)		(2) 55786.1 85.5	(1) 56042.5 43.0				
b <sup>2</sup> F' <sub>2</sub> .....		(55321.0) 55045.2 45.7	(0) 55001.5 00.5		(1) 55901.5 00.5	(1) 56067.0 67.3			
b <sup>2</sup> D <sub>3</sub> .....	(51860.8) (52273.3)			(3) 52595.3 95.3	(52852.9)		(48995.9)		
b <sup>2</sup> D <sub>2</sub> .....		(52127.7) (52452.5)			(0)		(48800.3) (48935.9)		
b <sup>2</sup> D <sub>1</sub> .....					52707.3 07.3				

TABLE VIII—Continued

	a <sup>1</sup> F <sub>4</sub>	a <sup>3</sup> F <sub>2</sub>	a <sup>3</sup> F <sub>4</sub>	a <sup>3</sup> D <sub>3</sub>	a <sup>3</sup> D <sub>5</sub>	a <sup>3</sup> D <sub>1</sub>	a <sup>3</sup> P <sub>2</sub>	a <sup>3</sup> P <sub>1</sub>	a <sup>3</sup> P <sub>0</sub>
b <sup>3</sup> P <sub>2</sub> .....	.....	.....	.....	$\left\{ \begin{array}{l} (\infty) \\ 58300.8 \\ 299.9 \end{array} \right.$	.....	$\left\{ \begin{array}{l} (\infty) \\ 58557.5 \end{array} \right.$	$\left\{ \begin{array}{l} (1) \\ 54700.4 \\ 00.5 \end{array} \right.$	$\left\{ \begin{array}{l} (0) \\ 54785.5 \\ 86.1 \end{array} \right.$	.....
b <sup>3</sup> P <sub>1</sub> .....	.....	.....	.....	.....	$\left\{ \begin{array}{l} (\infty) \\ 58435.8 \end{array} \right.$	$\left\{ \begin{array}{l} (\infty) \\ 58602.7 \end{array} \right.$	$\left\{ \begin{array}{l} (0) \\ 54578.8 \\ 78.8 \end{array} \right.$	$\left\{ \begin{array}{l} (0) \\ 54662.1 \\ 64.0 \end{array} \right.$	$\left\{ \begin{array}{l} (0) \\ 54662.1 \\ 58.5 \end{array} \right.$
b <sup>3</sup> P <sub>0</sub> .....	.....	.....	.....	.....	.....	$\left\{ \begin{array}{l} (\infty) \\ 58544.1 \end{array} \right.$	.....	$\left\{ \begin{array}{l} (0) \\ 54605.8 \\ 05.8 \end{array} \right.$	.....
a <sup>3</sup> S <sub>1</sub> .....	.....	.....	.....	.....	.....	.....	$\left\{ \begin{array}{l} (1) \\ 51831.2 \\ 31.0 \end{array} \right.$	$\left\{ \begin{array}{l} (\infty) \\ 51916.3 \\ 16.6 \end{array} \right.$	$\left\{ \begin{array}{l} (\infty) \\ 51910.4 \end{array} \right.$

TABLE VIII—Continued

	b <sup>3</sup> P <sub>2</sub>	b <sup>3</sup> P <sub>1</sub>	b <sup>3</sup> P <sub>0</sub>		a <sup>3</sup> P <sub>1</sub>	a <sup>3</sup> D <sub>2</sub> '	a <sup>3</sup> F <sub>3</sub>
a <sup>3</sup> D <sub>3</sub> .....	$\begin{Bmatrix} (2) \\ 99534 \\ 536 \end{Bmatrix}$	.....	.....	a <sup>3</sup> D <sub>2</sub> .....	$\begin{Bmatrix} (15) \\ 75321.7 \\ 23.1 \end{Bmatrix}$	$\begin{Bmatrix} (30) \\ 66726.7 \\ 24.8 \end{Bmatrix}$	$\begin{Bmatrix} (2) \\ 74642.5 \\ 44.0 \end{Bmatrix}$
a <sup>3</sup> D <sub>2</sub> .....	$\begin{Bmatrix} (00) \\ 99777 \\ 773 \end{Bmatrix}$	$\begin{Bmatrix} (1) \\ 99290 \\ 292 \end{Bmatrix}$	.....	b <sup>3</sup> D <sub>2</sub> .....	$\begin{Bmatrix} (6) \\ 43092.05 \\ 92.05 \end{Bmatrix}$	$\begin{Bmatrix} (10) \\ 33493.78 \\ 93.78 \end{Bmatrix}$	$\begin{Bmatrix} (15) \\ 41412.93 \\ 12.93 \end{Bmatrix}$
a <sup>3</sup> D <sub>1</sub> .....	.....	$\begin{Bmatrix} (0) \\ 99428 \\ 427 \end{Bmatrix}$	$\begin{Bmatrix} (0) \\ 99198 \\ 198 \end{Bmatrix}$	a <sup>3</sup> G <sub>4</sub> .....	.....	.....	$\begin{Bmatrix} (40) \\ 68718.1 \\ 18.1 \end{Bmatrix}$
				a <sup>3</sup> D <sub>3</sub> .....	.....	$\begin{Bmatrix} (0) \\ 36772.22 \\ 72.24 \end{Bmatrix}$	.....
				a <sup>3</sup> D <sub>2</sub> .....	.....	$\begin{Bmatrix} (3) \\ 36999.36 \\ 99.47 \end{Bmatrix}$	.....
				a <sup>3</sup> D <sub>1</sub> .....	.....	$\begin{Bmatrix} (3) \\ 37134.03 \\ 33.93 \end{Bmatrix}$	.....

Of the singlet terms,  $b^1D$  and  $a^1D'$  are confirmed by several intercombinations. There should be  $^1P$  and  $^1F$  terms to complete the triad, and, by analogy with *Sc* II, these should combine with  $b^1D$  and give strong lines not far from  $\lambda$  2400. Two strong lines of *Ti* III occur at  $\lambda$  2414 and  $\lambda$  2375, and nothing else remains unaccounted for in this part of the spectrum. There is a second  $^1D$  term in *Sc* II, intermediate in level between the  $^3F'$  and  $^3P'$  terms, and related to them. The corresponding term in *Ti* III should be much lower than that already found, and should combine with  $a^1P$  more strongly than with  $a^1F$ . After some searching, this was found. It combines with  $a^1P$ ,  $a^1D'$ ,  $a^1F$ , and  $a^3D_2$ . The first combination gives a strong line at  $\lambda$  1327.61, which was accidentally omitted from the original list, but is clearly due to titanium, as is confirmed by the close agreement of the observed and calculated positions.

A  $^1G$  term appears in *Sc* II, at a little higher level than  $a^3P'$  which combines with the  $^1F$  term to give a very strong line. The strong unclassified line of *Ti* at 1455 probably represents the same combination in *Ti* III. Though no other combinations with this level have been found, its reality is confirmed by the test depending on  $\sqrt{\nu/R}$  (see below). A low  $^1S$  term is also present in *Sc* II, combining with  $a^1P$  and  $a^3P$ , to give rather faint lines. Two lines at  $\lambda$  1495 and  $\lambda$  1433 show the right frequency difference, and about the right relative intensity. They have been inserted in the table, but are marked with a question, for the agreement may be accidental, and the resulting term value lies higher than might be expected.

All the stronger vacuum-spark lines of titanium have now been accounted for as belonging to *Ti* III or *Ti* IV. About 120 additional lines have been observed, of which only 11 have estimated intensities greater than 4. The three strongest are of intensity 10. Most, if not all, of these lines are probably due to *Ti* V.

Table IX gives all the lines which are known to belong to *Ti* III, including a few not appearing in the foregoing analysis, which are identified by their behavior in the spark and hot-spark. The wave-lengths shorter than  $\lambda$  2000 are from measures by the authors (almost all by Mr. Lang) on the Edmonton plates. For the longer wave-lengths, those marked (\*\*) have been measured for the first time on the Mount Wilson plates, and those marked (\*) remeas-



TABLE IX  
LINES OF TITANIUM III

$\lambda$ I.A.	Int.	$\nu$	Designation
Air			
**4215.55.....	5	23715.04	.....
**4207.54.....	3	23760.18	.....
**4204.95.....	2	23774.82	.....
**4200.11.....	2	23802.21	.....
2084.76.....	10	33493.78	$b^1D_2 - a^1D_1$
*2819.02.....	1	35462.90	$b^1D_2 - a^1D_1$
*2798.95.....	1	35717.65	$b^1D_2 - a^1F_2$
**2798.73.....	0	35719.97	$b^1D_2 - a^1D_1$
*2773.73.....	1	36041.90	$b^1D_2 - a^1F_3$
**2718.64.....	0	36772.22	$a^1D_3 - a^1D_1$
2701.95.....	1	36999.36	$a^1D_2 - a^1D_1$
2692.15.....	1	37134.03	$a^1D_1 - a^1D_1$
2580.43.....	5	38741.64	$a^1D_3 - a^1D_1$
2576.43.....	5	38801.79	$a^1D_2 - a^1D_1$
2567.53.....	8	38936.28	$a^1D_1 - a^1D_1$
2565.42.....	8	38968.31	$a^1D_2 - a^1D_1$
2503.42.....	15	38998.73	$a^1D_3 - a^1D_1$
**2556.58.....	1	39103.03	$a^1D_1 - a^1D_1$
**2548.69.....	1	39224.08	$a^1D_2 - a^1F_2$
**2548.55.....	1	39226.23	$a^1D_2 - a^1D_1$
*2547.98.....	0	39234.35	$b^1D_2 - a^1P_1$
*2542.41.....	1	39320.95	$a^1D_3 - a^1F_3$
2540.02.....	15	39357.96	$a^1D_1 - a^1F_2$
*2527.80.....	15	39548.20	$a^1D_2 - a^1F_3$
2516.01.....	20	39733.52	$a^1D_3 - a^1F_4$
2413.97.....	15	41412.93	$b^1D_2 - a^1F_3$
2375.02.....	6	42092.05	$b^1D_2 - a^1P_1$
2346.78.....	6	42598.52	$a^1D_3 - a^1P_2$
2339.01.....	5	42740.02	$a^1D_2 - a^1P_1$
2334.33.....	3	42825.71	$a^1D_2 - a^1P_2$
2331.67.....	3	42874.55	$a^1D_1 - a^1P_1$
2331.35.....	3	42880.45	$a^1D_1 - a^1P_0$
2327.04.....	1	42959.85	$a^1D_1 - a^1P_2$
2237.82.....	1	44672.43	.....
2199.30.....	1	45454.79	.....
Vacuum			
1957.02.....	00	51098.1	$a^1F_4 - a^1G_4$
1948.79.....	5	51313.9	$a^1F_4 - a^1G_3$
1941.40.....	4	51509.2	$a^1F_3 - a^1G_4$
1935.18.....	3	51674.8	$a^1F_2 - a^1G_3$
1929.34.....	1	51831.2	$a^1P_2 - a^1S_1$
1926.18.....	00	51916.3	$a^1P_1 - a^1S_1$
1901.31.....	3	52595.3	$a^1D_1 - b^1D_3$
1897.27.....	0	52707.3	$a^1D_1 - b^1D_2$
1832.21.....	0	54578.8	$a^1P_2 - b^1P_1$
1831.31.....	0	54605.8	$a^1P_1 - b^1P_0$
1829.42.....	0	54662.1	$\{a^1P_1 - b^1P_1$ $a^1P_0 - b^1P_1$
1828.14.....	1	54700.4	$a^1P_2 - b^1P_1$
1825.30.....	0	54785.5	$a^1P_1 - b^1P_1$

TABLE IX—Continued

$\lambda$ I.A.	Int.	$\nu$	Designation
Vacuum			
1811.09.....	2	55215.4	$a^3F_4 - b^3F_4'$
1797.69.....	1	55627.0	$a^3F_3 - b^3F_4'$
1797.10.....	0	55645.2	$a^3F_2 - b^3F_4'$
1792.56.....	2	55786.1	$\begin{cases} a^3D_3 - b^3F_3' \\ a^3F_2 - b^3D_2 \end{cases}$
1788.86.....	1	55901.5	$a^3D_2 - b^3F_3'$
1787.32.....	2	55949.7	$a^3D_1 - b^3F_4'$
1784.36.....	1	56042.5	$a^3D_2 - b^3F_3'$
1783.58.....	1	56067.0	$a^3D_1 - b^3F_3'$
1715.24.....	00	58300.8	$a^3D_1 - b^3P_2'$
1506.07.....	10	66398.0	$a^3P_1 - a^3D_1'$
1504.91.....	5D	66449.2	$a^3P_2 - a^3D_2'$
1504.59.....	10	66463.3	$a^3P_0 - a^3D_1'$
1502.36.....	10	66561.9	$a^3P_1 - a^3D_2'$
1499.17.....	20	66703.5	$a^3P_2 - a^3D_3'$
1498.65.....	30	66726.7	$a^3D_2 - a^3D_2'$
1496.59.....	1	66819.0	$a^3P_1 - a^3F_2$
1495.08.....	1	66886.0	$a^3S_0 - a^3P_1?$
1491.98.....	5	67025.0	$a^3P_2 - a^3F_3$
1455.22.....	40	68718.1	$a^3G_4 - a^3F_3$
1450.29.....	2	68951.8	$a^3D_2 - a^3D_3'$
1433.85.....	2	69742.3	$a^3S_0 - a^3P_1$
1424.14.....	20	70216.8	$a^3P_2 - a^3P_1$
1422.41.....	25	70303.2	$a^3P_2 - a^3P_2$
1421.69.....	20	70338.8	$\begin{cases} a^3P_1 - a^3P_1 \\ a^3P_1 - a^3P_0 \end{cases}$
1420.42.....	15	70401.7	$a^3P_0 - a^3P_1$
1420.04.....	15	70420.5	$a^3P_1 - a^3P_2$
1339.72.....	2	74642.5	$a^3D_2 - a^3F_3$
1327.60.....	15	75321.7	$a^3D_2 - a^3P_1$
1298.95.....	40	76985.3	$a^3F_3 - a^3D_2'$
1298.67.....	50	77001.9	$\begin{cases} a^3F_3 - a^3D_3' \\ a^3F_2 - a^3D_1' \end{cases}$
1295.91.....	30	77168.3	$a^3F_2 - a^3D_1'$
1294.67.....	50	77239.8	$\begin{cases} a^3F_3 - a^3D_3' \\ a^3F_3 - a^3F_2 \end{cases}$
1293.26.....	30	77323.9	$a^3F_4 - a^3F_3$
1291.64.....	20	77420.0	$a^3F_2 - a^3F_2$
1289.32.....	30	77560.2	$a^3F_3 - a^3F_3$
1286.38.....	40	77737.5	$a^3F_4 - a^3F_4$
1282.49.....	3	77973.3	$a^3F_3 - a^3F_4$
1008.08.....	0	99198	$a^3D_1 - b^3P_0$
1007.15.....	1	99290	$a^3D_2 - b^3P_1$
1005.75.....	0	99428	$a^3D_1 - b^3P_1$
1004.68.....	2	99534	$a^3D_3 - b^3P_2$
1002.23.....	00	99777	$a^3D_2 - b^3P_2$

ured there. The rest are Exner and Haschek's, reduced to the international scale.

A good test of the accuracy of the vacuum wave-lengths is afforded by the constant differences in the multiplets, since a number

of these are determined with high precision by means of the multiplets in the region of longer wave-length. The average residual  $O-C$  for all the lines involving the low terms  $a^3F'$ ,  $a^3P'$ , and  $a^3D$  is  $\pm 1.17$  frequency units, which corresponds to  $\pm 0.020$  Å. The largest residual, 0.08 Å, belongs to an unresolved double line; no other exceeds 0.05 Å. Since, on the average, these residuals correspond to differences from the mean of 3.5 quantities, the probable error of the measured wave-lengths would also be  $\pm 0.02$  Å, provided that all the errors arose from this source. They may actually be a little less. For the groups near  $\lambda 2500$ , involving the terms  $a^3D$  and  $b^3D$ , the average residual for 27 lines is 0.009 Å, giving a probable error rather less than  $\pm 0.01$  Å.

A few lines of longer wave-length, which appear in the spectrum of the Mount Wilson hot-spark between titanium electrodes and may belong to *Ti* III or *Ti* IV, but have not been classified, are given in Table X. None of these lines is visible in the ordinary spark.

TABLE X  
LINES PROBABLY BELONGING TO *Ti* III OR *Ti* IV

$\lambda$ Å.	Int.	$\nu$	$\lambda$ Å.	Int.	$\nu$
6202.43.....	2	15887.72	5812.01.....	4	17200.99
6246.56.....	2	16004.39	5801.27.....	6	17232.84
6243.47.....	2	16012.30	5722.72.....	2	17439.67
6234.46.....	0	16035.42	5695.97.....	10	17551.41
6231.10.....	0	16044.05	5306.80.....	5	18838.52
5889.69.....	2h	16974.13	5301.19.....	5	18858.45
5885.91.....	6	16985.03	5278.16.....	7	18940.74
5877.75.....	4	17008.60			

#### 6. THEORETICAL INTERPRETATION OF THE SPECTRUM OF *Ti* III

The doubly ionized atom of titanium has two electrons outside the complete "argon shell," and these alone are effective in producing the optical spectrum. These electrons may occupy orbits of types 4s, 4p, 3d, 4f, or others with higher total quantum numbers.<sup>1</sup> In *Ti* IV, where there is but one active electron, each orbit corresponds

<sup>1</sup> The word "orbit" is here used for convenience, to describe the corresponding feature of the atomic structure, with full recognition of the possibility of more complete interpretations in other terms. The notation 4s, 4p, and 3d is, by definition, exactly equivalent to Bohr's 4<sub>1</sub>, 4<sub>2</sub>, 3<sub>3</sub>, . . . , s, p, d, f, being substituted for the subscripts 1, 2, 3, 4.

to a single spectroscopic term of the same name,  $4S$ ,  $4P$ ,  $3D$ , etc. It is evident from the term values that, in this case, the  $3d$  electron is the most closely bound, next  $4s$ , then  $4p$ ,  $4d$ , etc.

We may therefore expect that the normal state of lowest energy in  $Ti$  III will be one in which both electrons are in  $3d$  orbits, which we may denote by  $(3d)^2$ . The spectroscopic terms which correspond to this atomic configuration are given by Hund's theory<sup>1</sup> as  $^3P'$ ,  $^3F'$ ,  $^1S$ ,  $^1D$ ,  $^1G$ , and of those the  $^3F'$  should lie the lowest.<sup>2</sup> The lowest term is actually of this type,  $a^3F'$ . The terms  $a^3P'$  and  $a^1D$  evidently arise also from this configuration, while the probable term  $a^1G$  and the suspected  $a^1S$  complete the group.

Next lowest in energy, but considerably higher, should be the configuration  $3d \cdot 4s$ , which should give rise to a  $^3D$  and a  $^1D$  term. These are evidently  $a^3D$  and  $b^1D$ .

None of the terms so far mentioned should combine with another to produce spectral lines, since such a transition would demand the shift of an electron from an  $s$  to a  $d$  orbit; but they should all combine (as far as their inner-quantum numbers permit) with the terms arising from the atomic configuration  $3d \cdot 4p$ , which can be reached from  $(3d)^2$  or  $3d \cdot 4s$  by "permissible" changes of an  $s$  orbit or a  $d$  orbit to a  $p$  orbit. This last configuration should give terms of the types  $^3P$ ,  $^3D'$ ,  $^3F$ ,  $^1P$ ,  $^1D'$ ,  $^1F$ . The terms called  $aP$ ,  $aD'$ , and  $aF$  in the triplet and singlet systems satisfy these conditions perfectly. The configuration  $4s \cdot 4p$  should give terms  $^3P$ ,  $^1P$ . These should combine strongly with those coming from  $4s \cdot 3d$ , and much less strongly with those of origin  $(3d)^2$ , for in the latter case one electron would have to jump from a  $d$  to an  $s$  orbit and the other from a  $d$  to a  $p$ , and such changes, though not impossible, are relatively unlikely.

The term  $b^3P$  meets these requirements. The corresponding singlet term has not been found.

The configuration  $3d \cdot 4d$  should give high-lying terms which combine with the  $P$ ,  $D'$ ,  $F$ , triads, at the middle level, but not with the low terms. Here Pauli's restriction is not operative, and we

<sup>1</sup> *Zeitschrift für Physik*, **33**, 345-371, 1925.

<sup>2</sup> The assignment of the accents follows Heisenberg's rule (*ibid.*, **32**, 859, 1925).

should expect S, P', D, F', G terms in both singlets and triplets. The full set of triplet terms has been found— $a^3S$ ,  $b^3P'$ ,  $b^3D$ ,  $b^3F'$ ,  $a^3G$ . The singlets should be much harder to identify and have not been detected.

All the observed terms in *Ti* III have now been interpreted. They are found to arise from just those atomic configurations which might be expected to give the stronger lines, and their relative energy levels are exactly what might be expected.

The configurations which should theoretically come next in importance are  $3d \cdot 5s$  and  $(4p)^2$ , the former giving  $^3D$  and  $^1D$  terms, and the latter  $^3P'$ ,  $^1S$ ,  $^1D$ . Three of these five terms have been identified in *Sc* II, and some of them may yet be found in *Ti* III.

The terms of origin  $(3d)^2$  and  $3d \cdot 4d$  represent the first two members of a series; but, as is shown by the analogy of *Sc* II, or, for that matter, of *Ti* IV, the Rydberg formula cannot safely be applied to them, for the binding energy of the low 3d electron is abnormally great, and the application of this formula leads to too high a limit for the series, while the series involving changes in an s electron gives a much better value.

The application of the simple Rydberg formula to the 3D and 4D terms in *Ti* IV leads to an ionization potential of 45.7 volts, 2.7 volts too high.

Similar treatment of the series in *Sc* II, beginning with the  $^3F'$ ,  $^3P'$ , and  $^1D$  terms of the  $(3d)^2$  configuration, gives ionization potentials of 13.7, 13.5, and 13.5 volts, as against 12.8 given by the more trustworthy series.

The uncorrected Rydberg formula therefore gives a result which is too high by 6 per cent for *Ti* IV and for *Sc* II also. If applied to the terms  $a^3F'$ ,  $b^3F'$  and  $a^3P'$ ,  $b^3P'$  of *Ti* III, it indicates that the limits of the series to which these terms belong, which is  $3^2D_3$  in *Ti* IV, lie at heights of 241,277 and 240,170 frequency units above the lowest level,  $^3F'_2$  in *Ti* III. The corresponding ionization potentials are 29.79 and 29.65 volts. On the assumption that the mean of these values is again 6 per cent too high, the true value of the ionization potential may be estimated as 28 volts, which is probably right within a volt or so.

7. COMPARISON OF *Ca* I, *Sc* II AND *Ti* III

The spectra of atoms comprising two or more spectroscopically active electrons can be compared as in section 4 by tabulating the values of  $\sqrt{\nu/R}$ . One precaution is necessary here, however, for which no need arose in the simpler case discussed in section 4. In that instance all the series converge toward a single limit, representing the normal energy state of the atom stripped down to the argon shell. In the general case the series fall into groups having different limits, corresponding to different states of the atom in the next higher degree of ionization. For example, starting with the configuration  $3d \cdot 4p$  of *Ti* III, the *p* electron may be shifted to  $5p$ ,  $6p$ , etc., orbits, while the other is unchanged, giving a series with the term  $3^2D$  of *Ti* IV as limit; or the *d* electron may be shifted, giving a quite different series, with the  $4^2P$  term as limit.

Every term of *Ti* III (and of all other similar spectra) therefore belongs to two series, which have different limits—with the exception of terms arising from configurations such as  $(3d)^2$ .

In general, it is advantageous to measure the value of  $\nu$  from the lower of these two limits; but, even so, this limit will not be the same in all cases. For example, for the  $3d \cdot 4p$  configurations of *Ti* III, it will be  $3^2D$  of *Ti* IV, for  $4p \cdot 4s$ ,  $4^2S$ ; and for  $(4p)^2$ ,  $4^2P$ . The ionization potential is usually measured from the state of lowest energy in one spectrum to that of lowest energy in the next—e.g., from  $^1S_0$  in *Ca* I to  $^2S_1$  in *Ca* II, from  $^3D_1$  in *Sc* II to  $^2D_2$  in *Sc* III, and from  $^3F_2$  in *Ti* III to  $^2D_2$  in *Ti* IV. The corresponding changes in electron configuration are from  $(4s)^2$  to  $4s$  in *Ca*,  $4s \cdot 3d$  to  $3d$  in *Sc*, and  $(3d)^2$  to  $3d$  in *Ti*. Care is therefore necessary in comparing different spectra to make sure that the values of  $\nu$  are actually measured from the proper limits.

For example, adopting the approximate value 28 volts derived above for the ionization potential of *Ti* III, it follows that the  $3^2D_2$  term of *Ti* IV lies higher than the base level  $a^3F_2$  of *Ti* III by 226,800 frequency units. For any term of *Ti* III arising from the configuration  $(3d)^2$ ,  $3d \cdot 4s$ , or  $3d \cdot 4p$ , the value of  $\nu$  may be found by subtracting the tabular energy level from this quantity. But for terms arising from  $4s \cdot 4p$  the limit is  $4^2S$  of *Ti* IV, which lies higher by 80,388 units; hence for these terms the tabular level must be sub-



tracted from 307,188. If, as is usually desirable, we take the component of greatest inner-quantum number in each term, we must also take the similar component of the limit, which makes the lower limit  $3^2D_3$  or 227,184. In view of the uncertainty of the estimate of the ionization potential, these figures will be rounded off in what

TABLE XI  
COMPARISON OF *Ca* I, *Sc* II, AND *Ti* III

CONFIGURATION	ELECTRON REMOVED	TERM	VALUES OF $\sqrt{\nu/R}$				
			<i>Ca</i> I	Diff.	<i>Sc</i> II	Diff.	<i>Ti</i> III
(3d) <sup>2</sup> .....	3d	<sup>3</sup> F' <sub>4</sub>	.....	.....	0.951	0.487	1.438
		<sup>3</sup> P' <sub>2</sub>	0.363	0.551	.914	.490	1.404
		<sup>1</sup> G <sub>4</sub>	.....	.....	.905	.487	1.392
		<sup>1</sup> D <sub>2</sub>	.372	.554	.926	.486	1.412
		<sup>1</sup> S <sub>0</sub>	.....	.....	0.919	.475?	1.394?
3d·4s.....	3d	<sup>3</sup> D <sub>3</sub>	.514	.573	1.087	.478	1.565
		<sup>1</sup> D <sub>1</sub>	.500	.577	1.077	.479	1.556
3d·4s.....	4s	<sup>3</sup> D <sub>3</sub>	.623	.351	0.974	.337	1.311
		<sup>1</sup> D <sub>1</sub>	.612	.351	.963	.337	1.300
3d·4p.....	4p	<sup>3</sup> F <sub>4</sub>	.497	.337	.834	.331	1.165
		<sup>3</sup> D' <sub>3</sub>	.475	.358	.833	.335	1.168
		<sup>3</sup> P <sub>2</sub>	.465	.359	.824	.330	1.154
		<sup>1</sup> F <sub>3</sub>	.453	.357	.810	.335	1.145
		<sup>1</sup> D' <sub>2</sub>	.498	.345	.843	.333	1.176
		<sup>1</sup> P <sub>1</sub>	.....	.....	.818	.325	1.143
3d·4d.....	4d	<sup>3</sup> G <sub>5</sub>	.....	.....	.631	.312	0.943
		<sup>3</sup> F' <sub>4</sub>	.....	.....	.607	.317	.924
		<sup>3</sup> D <sub>3</sub>	.323	.312	.635	.305	.940
		<sup>3</sup> P' <sub>2</sub>	.282	.318	.600	.312	.912
		<sup>3</sup> S <sub>1</sub>	.325	.301	.626	.300	0.926
4s·4p.....	4p	<sup>3</sup> P <sub>2</sub>	.557	.338	.895	0.346	1.241
		<sup>1</sup> P <sub>2</sub>	.483	.....	.....	.....	.....
(4p) <sup>2</sup> .....	4p	<sup>3</sup> P' <sub>2</sub>	0.574	0.331	0.905	.....	.....

follows to 227,000 and 307,000, corresponding to a principal ionization potential of 27.98 volts. For the term  $a^3P$ , for example, which arises from the configuration 3d·4p, the value of  $\nu$  is 227,000—81,024, or 145,976, while for  $b^3P$ , which arises from 4s·4p, it is 307,000—137,971 or 169,029.

In this way the values of  $\sqrt{\nu/R}$  given in Table XI have been derived. The terms are grouped according to the configuration from

which they arise and the character of the electron which is removed in passing to the limit. The data for *Sc* II are from Russell and Meggers,<sup>1</sup> those for *Ca* I from Russell and Saunders.<sup>2</sup> The differences in  $\sqrt{\nu/R}$  are very nearly the same for all the terms corresponding to the same electronic configuration. The reality of the low <sup>1</sup>G term in *Ti* III is thus satisfactorily confirmed. For the suspected <sup>1</sup>S term the difference is discordant, making its reality very doubtful. It is evident that a rather accurate prediction of the terms and principal lines in *V* IV could be made by extension of this scheme. Indeed, the value of the term *b*<sup>3</sup>P in *Ti* III, arising from the configuration 4s·4p, was predicted in this way, and the multiplet which depends upon it found near the predicted position.

The mean differences in  $\sqrt{\nu/R}$  for the related groups of terms are nearly the same as those for the corresponding terms for the one-electron systems, given in Table IV. Confining our attention to the terms produced by adding a given electron orbit to the normal state of the more highly ionized atom, we find:

Added Electron	Two-Electron Systems			One-Electron Systems		
	<i>Ca</i> I	<i>Sc</i> II	<i>Ti</i> III	<i>K</i> I	<i>Ca</i> II	<i>Sc</i> III
3d .....	0.551	0.487		0.535	0.470	
4s .....	.351	.337		.369	.326	
4p .....	.351	.332		.353	.319	
4d .....	0.310	0.306		0.334	0.296	

On the whole, the rate of diminution of the differences from the first column to the second is smaller for the two-electron systems. This may indicate that the assumed ionization potential for *Ti* III is a little too high. If it should be diminished by 0.5 volt, the mean differences in  $\sqrt{\nu/R}$  between *Sc* II and *Ti* III would become 0.474, 0.323, 0.316, and 0.285, respectively. The value 27.6 volts would give the best agreement.

The triplet separations remain to be considered. Landé has

<sup>1</sup> *Loc. cit.*

<sup>2</sup> *Astrophysical Journal*, 61, 1, 1925. Later work shows that the term there called 1p' is the <sup>1</sup>P' term arising from the configuration (4p)<sup>2</sup>; 2p' comes from (3d)<sup>2</sup>, and 3p' from 3d·4d, while the term there called q<sub>2</sub> is the <sup>3</sup>S term from the same configuration, and q<sub>1</sub> a component of the <sup>3</sup>D term of similar origin.

shown that his formulae for the doublets are applicable to the triplets as well, provided that the extreme separation of the outer com-

TABLE XII  
TRIPLET SEPARATIONS

Configuration and Terms		$\Delta\nu$	$n^*$	$10^4 \Delta N$	Mean	$Z_i$	$s$
Terms Involving a 4p Electron							
4s·4p.....	Ca I	158	1.796	419	.....	17.7	2.3
3p.....	Sc II	343	2.239	440	.....	18.2	2.8
	Ti III	709	2.396	461	.....	18.6	3.4
(4p) <sup>2</sup> .....	Ca I	134	1.739	323	.....	15.6	4.3
3P'.....	Sc II	346	2.206	417	.....	17.7	3.3
3d·4p.....	Ca I	6.7	2.011	25	.....	.....	.....
3P.....		66.7	2.105	284	356	16.4	3.6
3D'.....		166.3	2.152	759	.....	.....	.....
3F.....	Sc II	87	2.397	139	.....	.....	.....
		243	2.402	384	403	17.4	3.6
	Ti III	397	2.471	686	.....	.....	.....
		80	2.576	62	.....	.....	.....
		425	2.569	365	360	16.4	5.6
		737	2.600	653	.....	.....	.....
Terms Involving a 3d Electron							
4d·3d.....	Ca I	35.3	1.947	119	.....	16.4	3.6
3D.....	Sc II	168	1.842	120	.....	16.5	4.5
	Ti III	362	1.917	129	.....	17.1	4.9
4p·3d.....	Ca I	6.7	1.445	9	.....	.....	.....
3P.....		66.7	1.479	98	121	16.5	3.5
3D'.....		166.3	1.495	255	.....	.....	.....
3F.....	Sc II	87	1.777	56	.....	.....	.....
		243	1.779	156	157	18.8	2.2
	Ti III	397	1.790	260	.....	.....	.....
		80	2.077	36	.....	.....	.....
		425	2.074	192	189	20.7	1.3
		737	2.090	340	.....	.....	.....
(3d) <sup>2</sup> .....	Ca I	39.5	2.755	378	.....	.....	.....
3P'.....	Sc II	80.1	2.193	100	151	18.5	2.5
3F'.....		185	2.124	202	.....	.....	.....
	Ti III	185	2.122	90	142	17.9	4.1
		422	2.088	195	.....	.....	.....

ponents is taken. Slater<sup>1</sup> has shown that there is good reason to expect it to hold for terms arising from any configuration composed

<sup>1</sup> *Physical Review*, 28, 311, 1926.

only of  $s$  electrons, and electrons of any *one* other kind (e.g.,  $3d$  or  $4p$ ), except that the extreme separations for  $P, D, F, \dots$ , terms arising from the same configuration should be proportional to certain integers, which he takes as  $1, 2, 3, \dots$ , so that the mean of the separations for a triad such as  $P, D', F$ , should be equal to that for the  $D'$  term. For configurations involving electron orbits, other than  $s$  orbits, of two different sorts, his formulae are much more complicated.

The results derived in this way from the three spectra now under consideration are given in Table XII. The  $3d \cdot 4p$  configuration is here presented in a double rôle, as arising from the addition of a  $4p$  electron to a previously existing  $3d$  state, and vice versa. The values of  $n^*$  are of course quite different in the two cases. The individual values of  $\Delta n$  are rather ragged, but if the mean is taken for the triad, and this is treated as if it arose from a single electron of the type which has been supposed to be added in forming the configuration, the resulting mean values of  $\Delta n$ , and those of  $s$  derived from them, are in surprisingly good agreement with the others. This, however, means little more than that the mean separations of the terms arising from the simpler and more complex configurations are of about the same size. The  ${}^3F'$  and  ${}^3P'$  terms of origin  $(3d)^2$  have been treated in the same way. The irregularity of the individual values is so great as to make it evident that a great deal more work must be done before a satisfactory theory of the term separations in such cases can be reached.

In conclusion, we take much pleasure in expressing once more our thanks to Dr. Anderson and Miss Carter for the observational material upon which much of the present investigation has been based.

PRINCETON UNIVERSITY OBSERVATORY  
UNIVERSITY OF ALBERTA  
April 1927

## TRANSMISSION PROPERTIES OF SOME FILTERS<sup>1</sup>

By EDISON PETTIT

### ABSTRACT

*Determination of transmissions.*—The determinations between  $\lambda$  0.23 and 0.45  $\mu$  were made photographically with a 1-m concave grating spectrograph; those to the red of  $\lambda$  0.45  $\mu$  were made with a monochromatic illuminator and vacuum thermocouple.

*Standards of wave-length in the infra-red.*—A table of wave-lengths of easily recognized features of *absorption spectra* is given for the region  $\lambda$  0.74 to 2.1  $\mu$ , which may be used where accuracy greater than 0.01  $\mu$  is not required.

*Transmission data.*—The transmission curves of 44 filters are given from  $\lambda$  0.23 to 2.3  $\mu$ , and in several cases to greater wave-lengths in the infra-red.

*Photo-chemical effects.*—The effect of sunlight on green celluloid, glass, silver, and gold films has been studied. Solarized green celluloid is a valuable filter transmitting the infra-red with an efficiency of 80-90 per cent, has a sharp cut-off at  $\lambda$  0.7  $\mu$ , and transmits nothing from this point to  $\lambda$  0.23  $\mu$ .

During several years past the writer has had occasion to test the properties of transmission of a number of filters in connection with measurements of radiation. These have been collected and are given here in the form of plotted curves. Gibson<sup>2</sup> has recently compiled a list of such curves, a few of which were re-determined and are included in this collection, since the present results extend much farther into the infra-red. As the curves extend from  $\lambda$  0.2 to 2.3  $\mu$  and beyond, they should be of some interest to those engaged in photography and spectroscopy, in either ultra-violet or infra-red.

### DETERMINATIONS IN THE ULTRA-VIOLET

The determination of transmissions to the violet of  $\lambda$  0.45  $\mu$  was made photographically with a 1-m concave grating ruled by Jacomini with shallow lines. This was mounted in Littrow form and was used in the first order, giving a dispersion of 17.4 A per millimeter. The plateholder was so arranged that fifteen exposures could be put on each plate. Cramer contrast plates were used, as the time-intensity coefficient is nearly unity.

The image of an iron arc was projected upon the slit by a quartz lens. Exposures of 50 and 20 seconds were made through the filter,

<sup>1</sup> Contributions from the Mount Wilson Observatory, Carnegie Institution of Washington, No. 336.

<sup>2</sup> *Journal of the Optical Society of America*, 13, 267, 1926.

and exposures of 20 to 1 seconds by steps of 2 seconds were made without the filter. The former were cut off the plate and the line intensities compared under a magnifier with those of the latter. Transmissions from  $\lambda$  0.45 to 0.23  $\mu$  were thus obtained with ease. In one or two cases a spark between silver electrodes was used to extend the transmission curve to the violet of  $\lambda$  0.23  $\mu$ .

For very low transmissions, such as are found in metallic films, non-adjustable sectors having factors of 0.10 and 0.05 were used to reduce the free exposures. These sectors were 15 inches in diameter and were driven at a considerable speed. The geometric and photometric factors were found to be practically identical.

#### DETERMINATIONS IN THE VISUAL AND INFRA-RED REGIONS

Most of the measurements for wave-lengths greater than 0.45  $\mu$  were made with a Hilger constant-deviation spectroscope arranged as a monochromatic illuminator. The source of radiation was a nitrogen lamp of the straight-filament street-lighting type, run with 30 per cent overload, an image of the filament being formed on the first slit by a lens. The radiation from the second slit was focused upon one junction of a compensated vacuum-thermocouple by means of a convex lens of 1-inch focal length. This arrangement is more efficient than a thermopile placed immediately behind the second slit, but is somewhat slower. A moving-coil galvanometer was used, an image of a filament being projected on a scale, the deflections being kept near 100 mm.

The widths of the slits were kept the same, being approximately  $0.0015 \times \mu$  at  $\lambda$  0.5  $\mu$ ,  $0.0045 \times \mu$  at  $\lambda$  1.0  $\mu$ ,  $0.008 \times \mu$  at  $\lambda$  1.5  $\mu$ , and  $0.020 \times \mu$  at  $\lambda$  2.0  $\mu$  where  $\mu$  indicates the wave-length. For wave-lengths greater than 2.5  $\mu$  a rocksalt monochromatic illuminator was used with concave mirrors throughout. A six-junction thermopile was employed with this instrument, and the source of radiation was a heated platinum strip or Nernst glower.

In both instruments the filter was placed either in front of the first slit or behind the second, the change in focus being of no importance; hence collimation of the light passing through the filter was unnecessary.



## DISPERSION IN THE INFRA-RED

The dispersion curve of the Hilger instrument could not be computed, as the properties of the glass were unknown, hence standards were sought in the infra-red. For a first approximation the atmospheric absorption bands and sodium emission lines were used. After

TABLE I  
WAVE-LENGTHS OF THE PRINCIPAL FEATURES OF ABSORPTION SPECTRA

$\lambda$	Substance	Thickness in Milli- meters	Feature	Transmis- sion	Figure	Curve
0.740 $\mu$ ...	Didymium	8.8	Min.	0.05	2	4
0.740.....	Neodymium	5	Min.	.03	2	3
0.770.....	Didymium, Neodymium	.....	Max.	.58, .80	.....	.....
0.800.....	Neodymium	.....	Min.	.03	.....	.....
0.805.....	Didymium	.....	Min.	.01	.....	.....
0.830.....	Neodymium	.....	Max.	.85	.....	.....
0.845.....	Didymium	.....	Max.	.63	.....	.....
0.865.....	Neodymium	.....	Min.	.16	.....	.....
0.880.....	Didymium	.....	Min.	.18	.....	.....
0.940.....	H <sub>2</sub> O	10	V slope	.70	3	5
0.975.....	H <sub>2</sub> O	10	Min.	.55	.....	.....
1.000.....	H <sub>2</sub> O	10	R slope	.62	.....	.....
1.065.....	Didymium	8.8	Min.	.53	.....	.....
1.110.....	Benzol	10	V slope	.60	1	1
1.130.....	H <sub>2</sub> O	10	V slope	.50	.....	.....
1.135.....	Benzol	10	Min.	.20	.....	.....
1.160.....	Benzol	10	R slope	.60	.....	.....
1.225.....	Didymium	8.8	Min.	.54	.....	.....
1.350.....	H <sub>2</sub> O	10	V slope	.09	.....	.....
1.350.....	H <sub>2</sub> O	5	V slope	.28	2	3
1.430.....	Benzol	10	Min.	.61	.....	.....
1.520.....	Didymium	8.8	Min.	.26	.....	.....
1.610.....	Benzol	10	V slope	.50	.....	.....
1.680.....	Benzol	10	Min.	.03	.....	.....
1.700.....	Didymium	8.8	Max.	.62	.....	.....
1.800.....	Benzol	10	R slope	.26	.....	.....
1.920.....	Didymium	8.8	Min.	.31	.....	.....
1.970.....	Benzol	10	Max.	.42	.....	.....
2.100.....	Benzol	10	V slope	0.23	.....	.....

smoothing by a number of determinations, the transmission-curves for benzol 1 cm and glycerine 1 cm were run and compared with the curves obtained by Coblenz.<sup>1</sup>

Figure 1 shows how these curves agree, the dotted curves being due to Coblenz. An interesting feature of the curve for benzol is the sharp absorption band at  $\lambda 1.135 \mu$ . As the crosses indicate, the

<sup>1</sup> *Scientific Papers of the Bureau of Standards*, 17, 267, 1922.

observations of Coblentz were made on the edges of the band, which was therefore drawn much too shallow. This band serves as a convenient standard of wave-length.

Aside from narrow absorption bands, the edges of wide bands with steep sides may be used for calibration purposes. A list of standards available in the absorption spectra observed in the course of the present work is listed in Table I. The point referred to is indicated on the corresponding curve by the letter *S*. The data in the table will be useful in securing dispersion curves in the infra-red where accuracy greater than about 0.01 is not desired.

#### THE TRANSMISSION CURVES

The curves of similar transmission features have been grouped in Figures 1-9. Data concerning each curve appear opposite its symbol in the margin of each plot. In the case of solutions of salts, the mass of crystalline salt per square centimeter in the optical path is given, since the water plays little part in the form of the curve to the violet of  $1\ \mu$ , and the form to the red of this is the typical (OH) absorption.

Table II is a key to the various curves and will assist in identification.

#### PHOTO-CHEMICAL EFFECTS

The transmission curve of green celluloid is shown in Figure 4, curve 10. This screen, on exposure to sunlight for a period of two months, turns nearly black, transmitting only a dull-red light. The transmission curve for this solarized green celluloid is practically identical with that of ordinary green celluloid in the infra-red from  $\lambda\ 0.7$  to  $2.0\ \mu$ , the transmission bands in the green  $\lambda\ 0.50\ \mu$  and ultra-violet  $\lambda\ 0.36\ \mu$  being completely suppressed.<sup>1</sup> This solarized celluloid forms the only screen, to the writer's knowledge, which has a sharp cut-off at  $\lambda\ 0.7\ \mu$ , transmits no radiation from this point to  $\lambda\ 0.23\ \mu$ , and transmits the infra-red beyond  $\lambda\ 0.7\ \mu$  with an efficiency of 80-90 per cent. This should be of interest to those working in spectroscopy and photography in the infra-red.

<sup>1</sup> *Publications of the Astronomical Society of the Pacific*, 39, 170, 1927.

TABLE II

Filter	Thickness in Millimeters	Cell	Wall Thickness in Milli- meters	Figure	Curve
Acetic acid, glacial.....	10	Quartz	5	9	37
Alum, crystal.....	1.65			7	34
Asphalt (Abbot).....		Glass		9	47
Asphalt.....	0.090	Glass	0.6	7	26
Benzol.....	10	Quartz	5	7	30
Bottle glass.....	4			1	1
Bottle glass solarized.....	4			7	29
				7	28
				9	49
Celluloid, green.....	0.25			4	10
Copper ammonium sulphate*.....	8	Glass	2	3	9
Corning G 24 (red).....	6			4	14
G 38 (noviol).....	3.93			4	13
124 J (heat absorbing).....	1.17			6	20
124 J (heat absorbing).....	4.85			6	21
G 555 Q (didymium).....	8.8			2	4
G 585 M (blue-purple ultra).....	3.52			5	16
G 980 A (ultra-violet clear).....	4.10			9	46
G 984 B (green).....	3.95			4	15
G 985 B (ultra-violet).....	4.97			5	17
Uviol.....	4.25			7	27
				9	39
Glycerine.....	10	Quartz	5	1	2
Gold film.....	Thin	Quartz	5	6	23
Gold film.....	Thick	Quartz	1	6	24
Gold.....	2 Thick films	Quartz	1	6	25
Iceland spar.....	1.67			8	36
				9	48
Malachite green†.....	30	Glass	5	3	8
Microscope cover-glass.....	0.165			8	35
				9	45
Neodymium chloride‡.....	5	Glass	2	2	3
Photographic plate, Clear.....		Glass		7	31
Photographic plate, Fogged.....		Glass		7	33
Photographic plate, Ratio Fogged/Clear.....		Glass		7	32
Plate glass.....	6.5			9	40
Pulkowa B 67.....	3.52			4	11
Pulkowa B 68.....	3.55			4	12
Quinine sulphate§.....	10	Quartz	5	9	38
Silver film.....	Thin			9	41
Silver film.....	Thick			9	42
Silver film.....	2 Thick films			9	43
Spencer (heat absorbing) 4110.....	2.85			6	22
Vitaglass.....	2.56			9	44
Water.....	10	Quartz	5	3	5
Water (old).....	10	Glass	0.165	3	6
Water.....	10	Glass	0.165	3	7
Wratten W 13.....	4.26			5	19
Wood's filter glass.....	1.72			5	18

\* Mass per cm<sup>2</sup> = 17 mg. † Mass per cm<sup>2</sup> = 0.4 mg. ‡ Mass per cm<sup>2</sup> = 43 mg. § Mass per cm<sup>2</sup> = 3 mg.

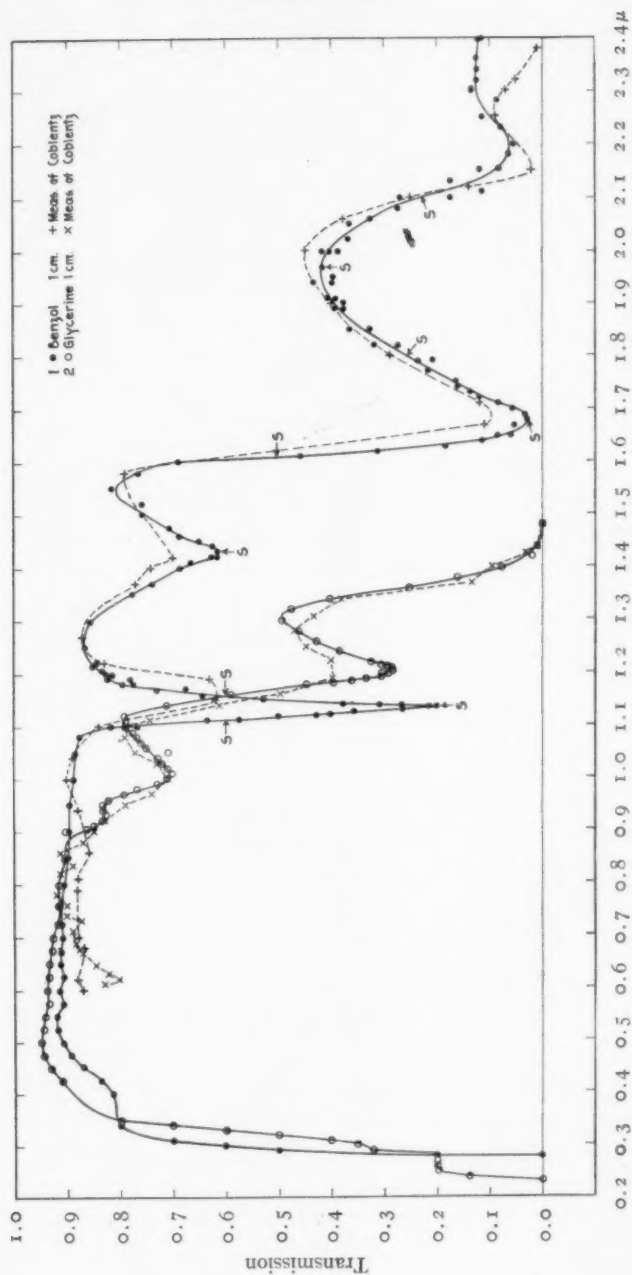


FIG. 1

# TRANSMISSION OF FILTERS

49

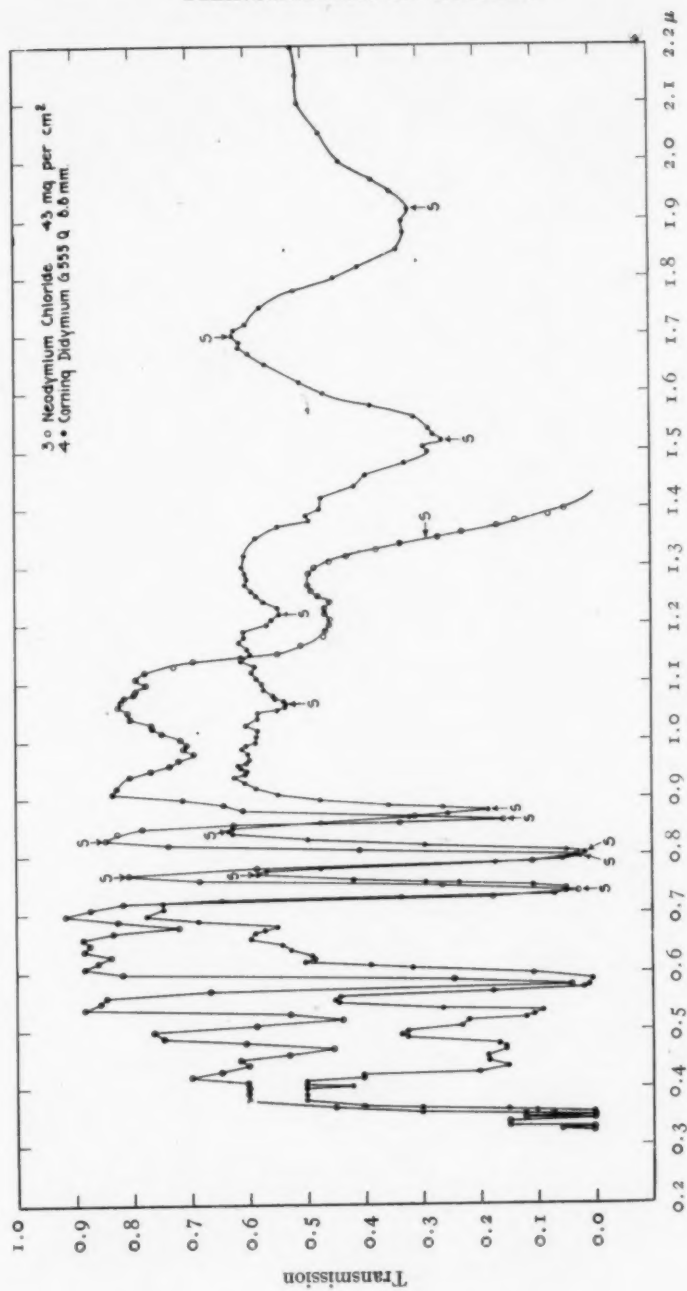


FIG. 2

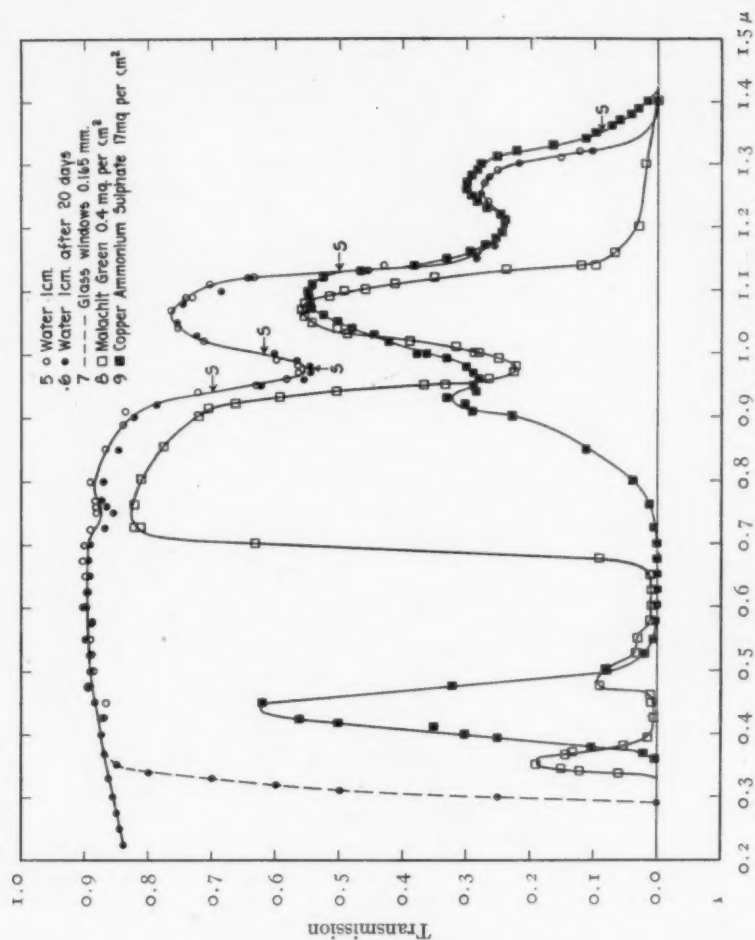


FIG. 3



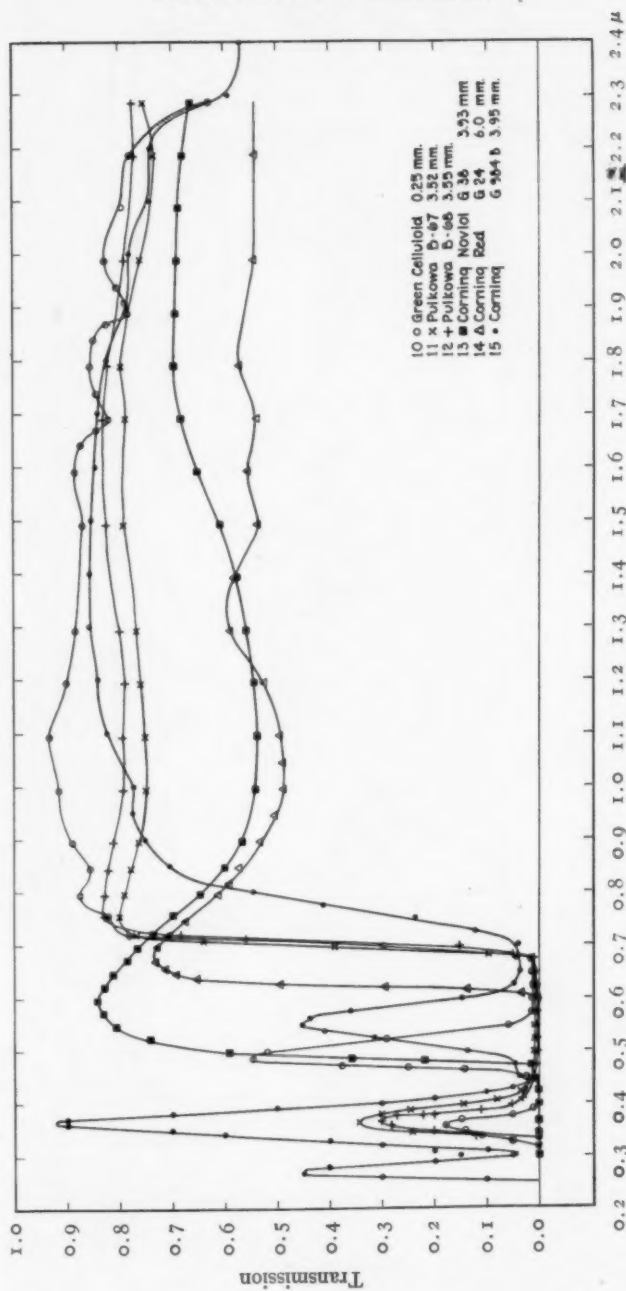


FIG. 4

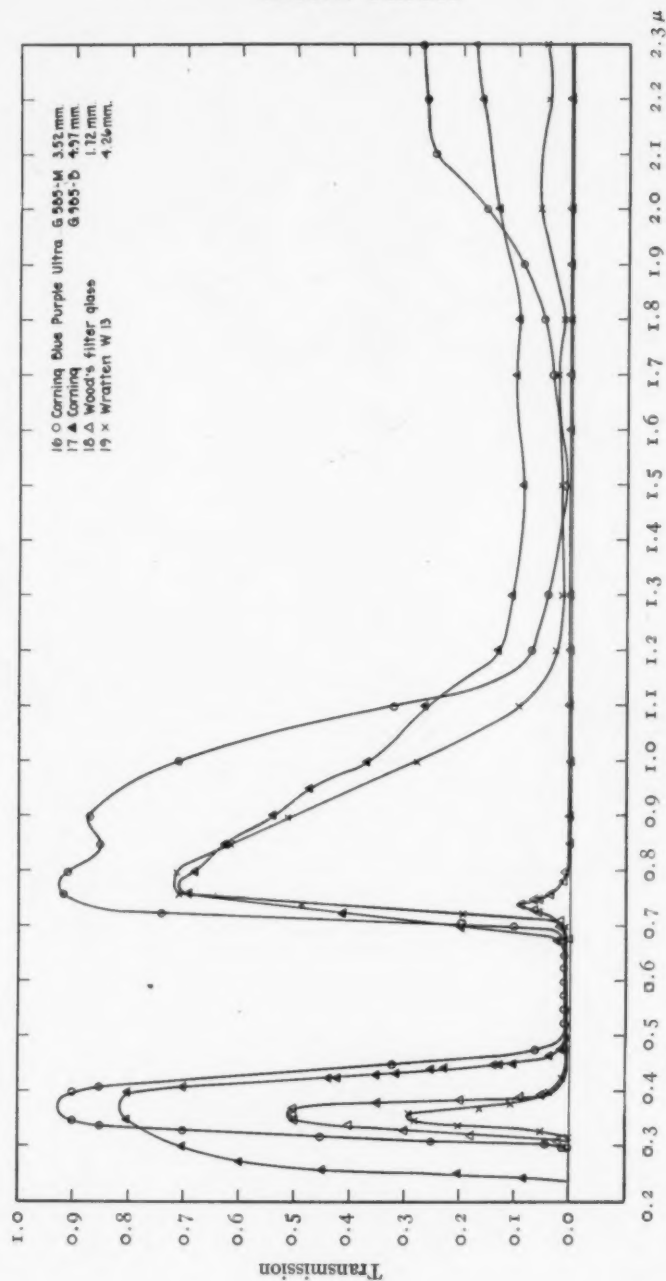


FIG. 5

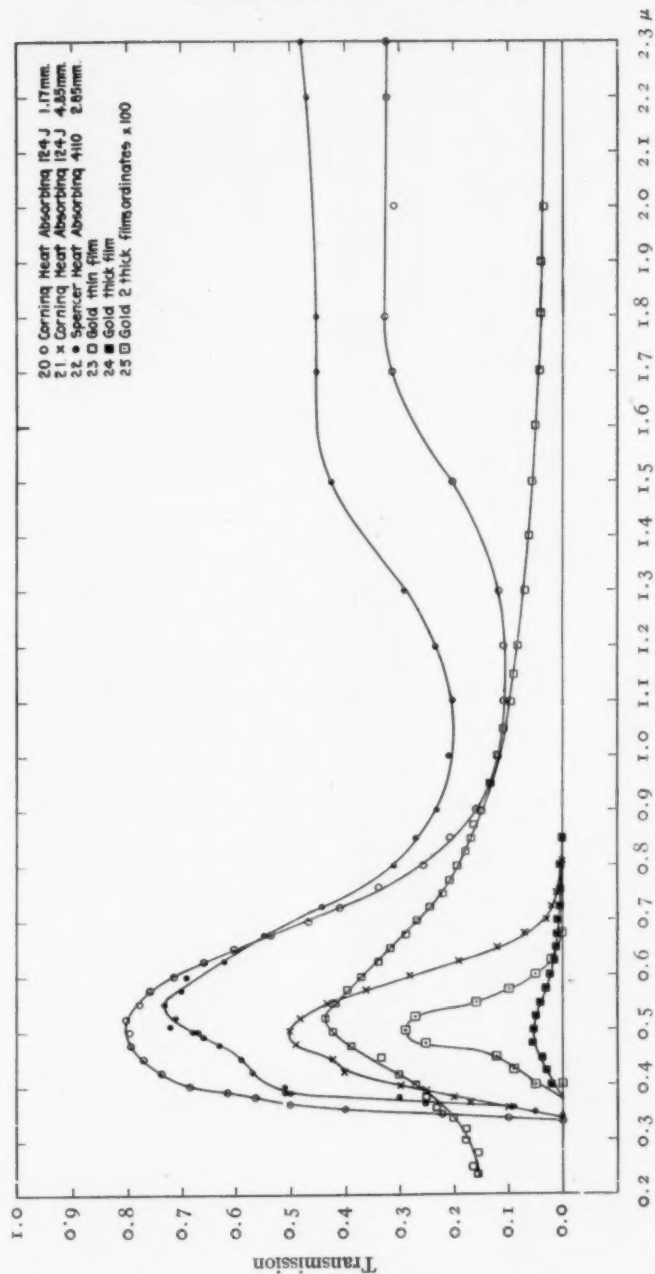


FIG. 6

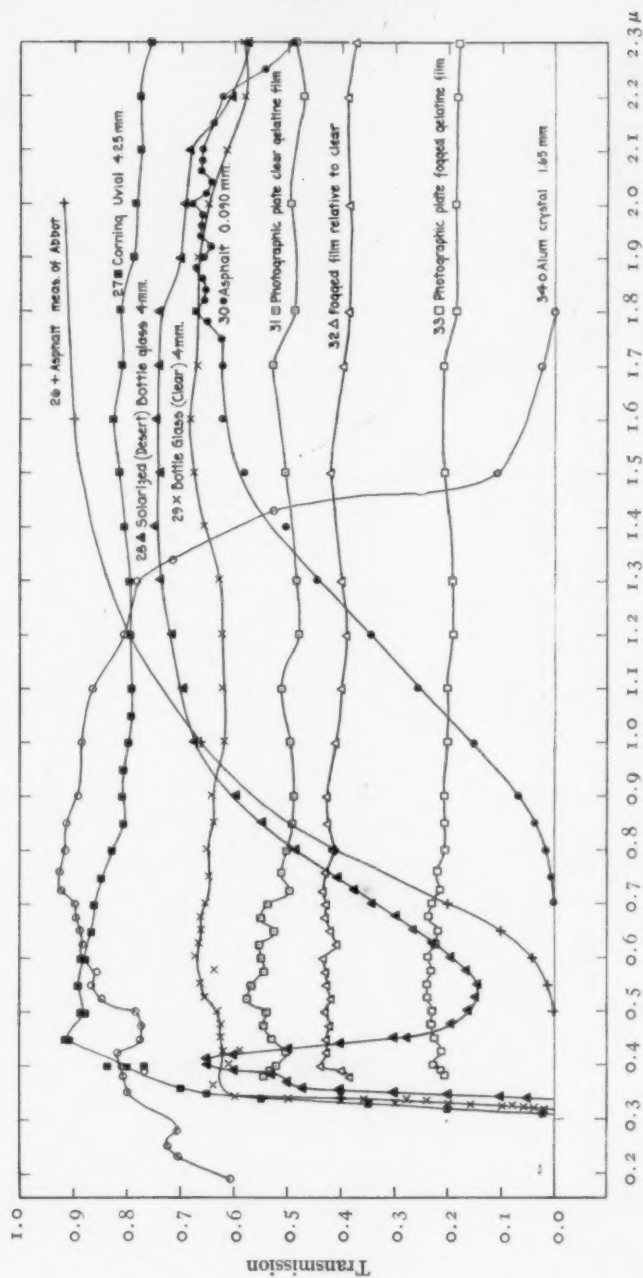


FIG. 7

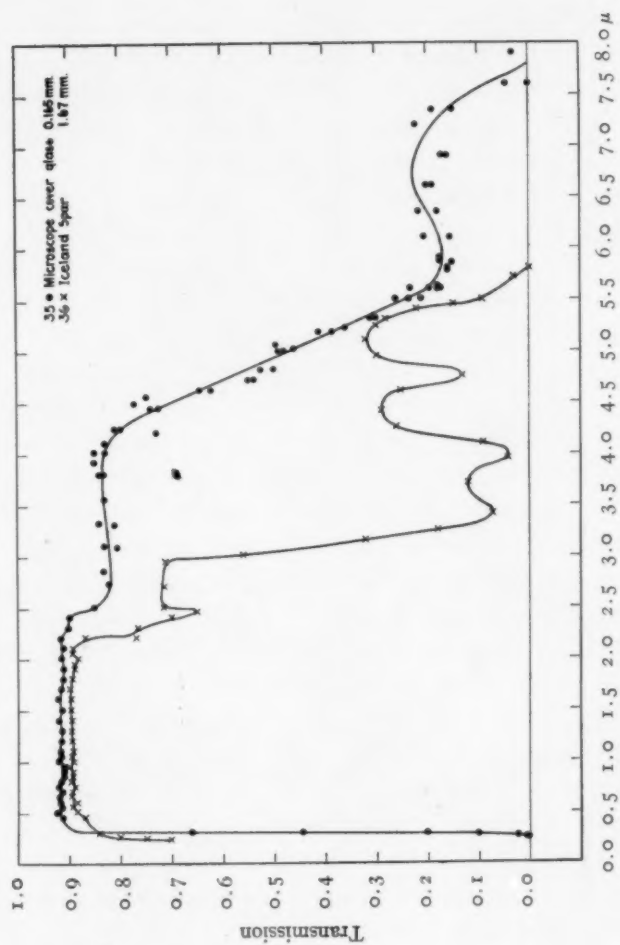


Fig. 8

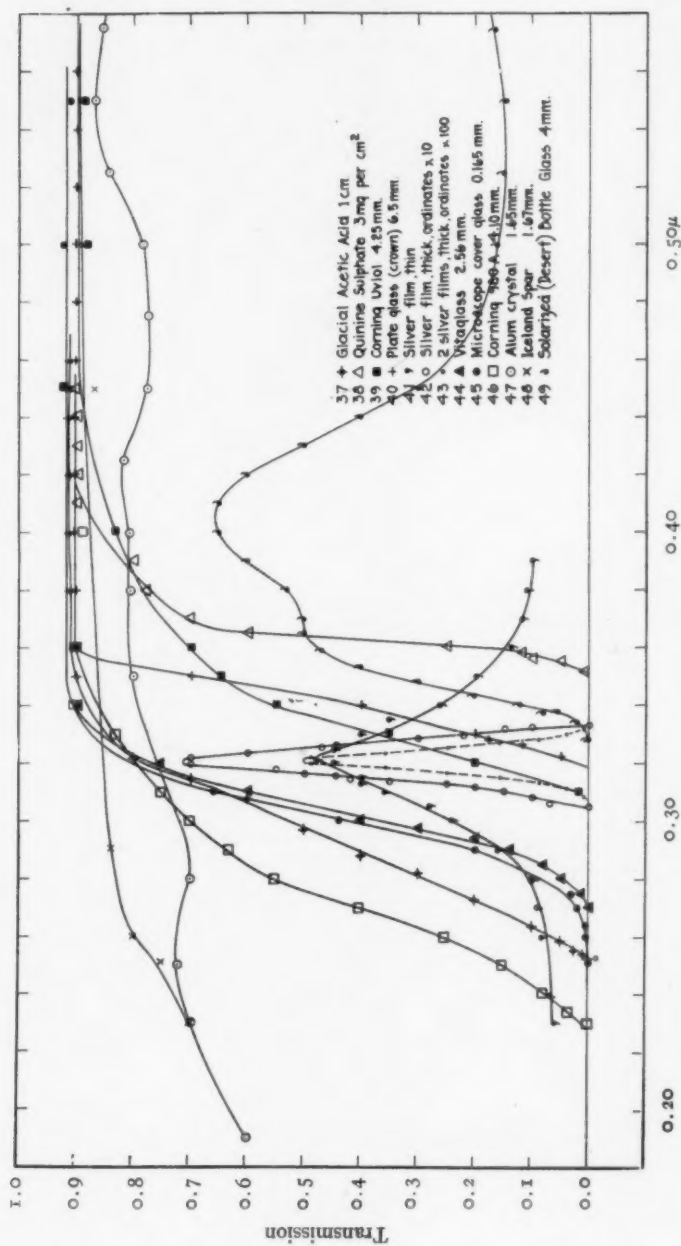


Fig. 9



Photo-chemical effects of sunlight on glass are especially important in the study of solar radiation. Curve 29, Figure 7, is the transmission of an ordinary colorless bottle, and curve 28, Figure 7, is the transmission of a bottle picked up at the New Dale mining camp in the Mojave Desert. The bottle had turned a dark-violet tint, and its age may be judged from the fact that this mining camp has been abandoned for eleven years. The wave-length of the radiation producing this violet tint must be greater than  $0.33 \mu$  approximately, since this and a number of other such bottles examined by the writer are almost uniformly colored throughout, showing only a slightly deeper tint on the side exposed to the sun. It is probable that the effect is practically confined to the region  $\lambda$   $0.33$  to  $0.45 \mu$ , where the transmission is high.

Pieces of window-glass found at the same place showed no tendency to color; and no specimen of window, plate, or optical glass showing this tint has been brought to the writer's attention. It is probable that the violet tint produced by sunlight is due to the manganese dioxide used to decolorize bottle glass, and does not appear in glass not treated with this substance. Such objectives as the Yerkes 40-inch, and those in the tower telescopes, which are much exposed to sunlight, show no trace of color due to solarization.

That the transmissions of the gold and silver films used in the ultra-violet solar radiometer are not affected by sunlight has already been pointed out.<sup>1</sup> These films are on the inside of the lens cells and protected from the air. After a period of more than two-and-a-half years these films show no change in transmission between the exposed portions and that behind the diaphragm, and no trace of tarnish. A case of tarnish on silver, apparently due to photo-chemical effects, was observed, however, in the coelostat of the Snow telescope. A 12-inch diaphragm was put on the 30-inch coelostat mirror after freshly silvering. After a few days the exposed area of the mirror became tarnished a brown color, while the remainder of the mirror was unaffected. The 24-inch fixed flat, which had no diaphragm, also showed tarnish over an area 12 inches in diameter where a spot of light from the coelostat was received. This tarnish was probably due to insufficient cleaning of the silver film

<sup>1</sup> *Proceedings of the National Academy of Sciences*, 13, 380, 1927.

after being deposited, and is not ordinarily seen in mirrors used for solar investigations.

There is a current opinion that a silver film through which the sky can be easily seen transmits nearly 100 per cent at  $\lambda 0.32 \mu$ . Such films of chemically deposited and sputtered silver were tested and found to transmit only 8 per cent. Curve 41, Figure 9, is for a chemically deposited film, so thin that it is nearly colorless, and that not only the sky but objects at a distance are easily distinguishable. Its transmission at  $\lambda 0.32 \mu$  is only 48 per cent. There appears to be little difference in this respect between chemically deposited and sputtered films.

Visual-light values can be obtained with radiometric apparatus by passing the source of light through a combination of green celluloid and Corning 124 J, about 4 mm thick. The efficiency of this screen is only 25-30 per cent, but it may prove useful under certain circumstances.

The writer is indebted to Mr. Nicholson for assistance in obtaining curves 35 and 36, and to Miss Richmond and Miss Ware for assistance in the computation of transmissions.

CARNEGIE INSTITUTION OF WASHINGTON  
MOUNT WILSON OBSERVATORY  
May 1927

## THE NEBULOUS ENVELOPE AROUND NOVA AQUILAE NO. 3<sup>1</sup>

BY EDWIN HUBBLE AND JOHN CHARLES DUNCAN

### ABSTRACT

*Expanding envelope of Nova Aquilae No. 3 (1918).*—Photographs made with the 100-inch reflector at Mount Wilson shows a nebulous disk around the nova, which expanded perceptibly during the interval of eleven months covered by the observations. Measures at four epochs give a mean diameter of 16".4 corresponding to the mean epoch, September 21, 1926.

This indicates an angular increase in the radius of the expanding disk or shell of nebulosity of 1".0 per year, which is consistent with the earlier micrometric measures of the visual envelope. A comparison with the linear rate of expansion, 1700 km/sec. as derived from early spectrograms, leads to a distance of 360 parsecs;  $\pi = 0''.0028$ .

Slitless spectrograms show a strong image of the disk at  $\lambda$  4686, slightly weaker images at  $H\beta$ ,  $H\gamma$ , and  $H\delta$ , and traces at  $N$ , and  $\lambda$  4363.

The outburst of Nova Aquilae No. 3 (1918) was first observed early in June, 1918. By October of the same year, Barnard had detected and measured a bright nebulous envelope about two-thirds of a second of arc in diameter, symmetrically distributed around the star. This envelope expanded steadily and gradually faded until it could no longer be observed with visual refractors. Both Barnard<sup>2</sup> and Aitken<sup>3</sup> measured the diameter as long as this could be done with confidence. The last-published value is that of Aitken,<sup>3</sup> 5".0, on July 7, 1921, some three years after the outburst.

Photographs with the 100-inch reflector at Mount Wilson in the early summer of 1926 brought the envelope once more under direct observation. It had continued to expand (and probably to grow fainter)<sup>4</sup> until, at that time, its diameter was about 16". The envelope photographs as a uniform disk with a sharp and sensibly circular edge. The star is central, as nearly as can be determined. The object has the appearance of a planetary nebula in which the central star is unusually bright.

<sup>1</sup> Contributions from the Mount Wilson Observatory, No. 335.

<sup>2</sup> *Astrophysical Journal*, 49, 199, 1918; *Publications of the Astronomical Society of the Pacific*, 32, 222, 1920.

<sup>3</sup> *Publications of the Astronomical Society of the Pacific*, 36, 283, 1919; 32, 231, 1920; 33, 219, 1921.

<sup>4</sup> In July, 1926, the envelope was invisible under favorable conditions at the primary focus of the 100-inch reflector.

Exposures on Eastman 40 plates, ranging from a few seconds up to sixty-five minutes, indicate that a limiting exposure of about two minutes is necessary to register a trace of the envelope; but that once impressed, its diameter does not materially increase with increasing exposure. On the short exposures there is a slight brightening at the rim, consistent with the theory that the envelope is a shell of material thrown off from the star at the time of the outburst. The limiting exposure corresponds to a surface brightness of the order of 18.0 in photographic magnitudes per square second of arc.<sup>1</sup> This, combined with the area, leads to a total magnitude of the order of 12.3. The central star was estimated as about 10.5.

The measures of the diameter of the envelope are given below. Each value represents the mean of two plates and has a probable error of the order of 0".2.

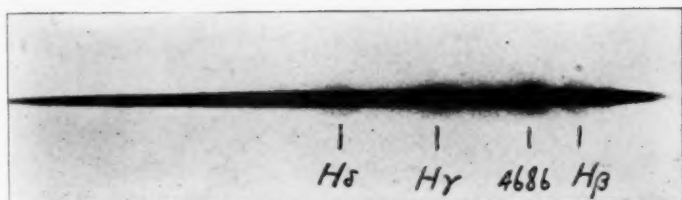
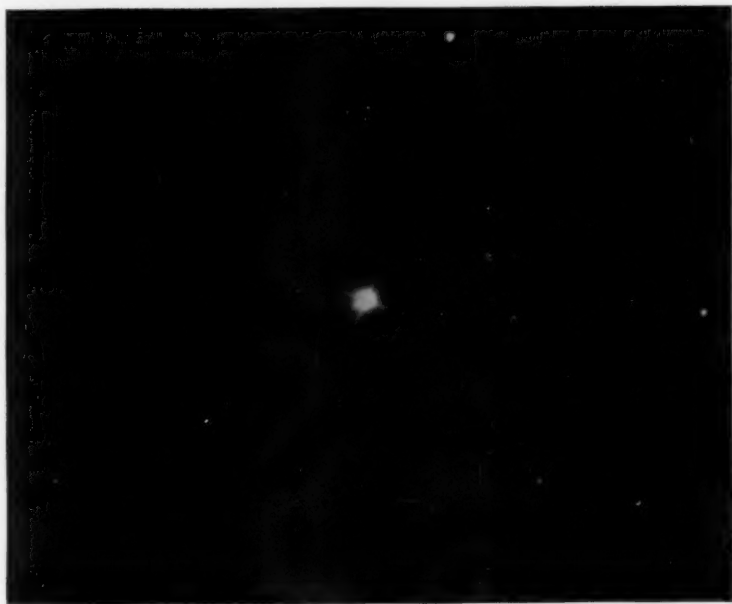
May 17, 1926.....	15".7
July 13, 1926.....	15.9
Sept. 4, 1926.....	16.4
April 25, 1927.....	17.6
Mean (Sept. 21, 1926).....	16.4

On the assumption that the expansion has proceeded at a uniform rate since the initial outburst, the rate of increase in the radius is approximately 1".0 per year. The early visual measures of Barnard and of Aitken, with the exception of the last one by Aitken, are consistent with this interpretation. The discordant measure was made in July, 1921, and hence, for a rate of 1".0 annually, should have given a diameter of about 6".1. It was in fact about 5".0.

Since it is improbable that the velocity of expansion has been accelerated since 1921, it seems easier to account for the discrepancy as due either to the faintness of the object or to differences in the size of the visual and photographic images. In 1920, for instance, the light appears to have been largely concentrated in the  $N_1$  and  $N_2$  images, while in 1926 these were inconspicuous, and most of the light came from the Balmer lines of hydrogen and  $\lambda$  4686. Slitless spectrograms made in August, 1926, at the primary focus of the 100-inch

<sup>1</sup> Seares has determined the limiting surface brightness which will register in an exposure of one minute on Seed 30 plates with a reflector of focal ratio 1:5, as  $18.8 \pm 0.3$  pg. mag. per square second.

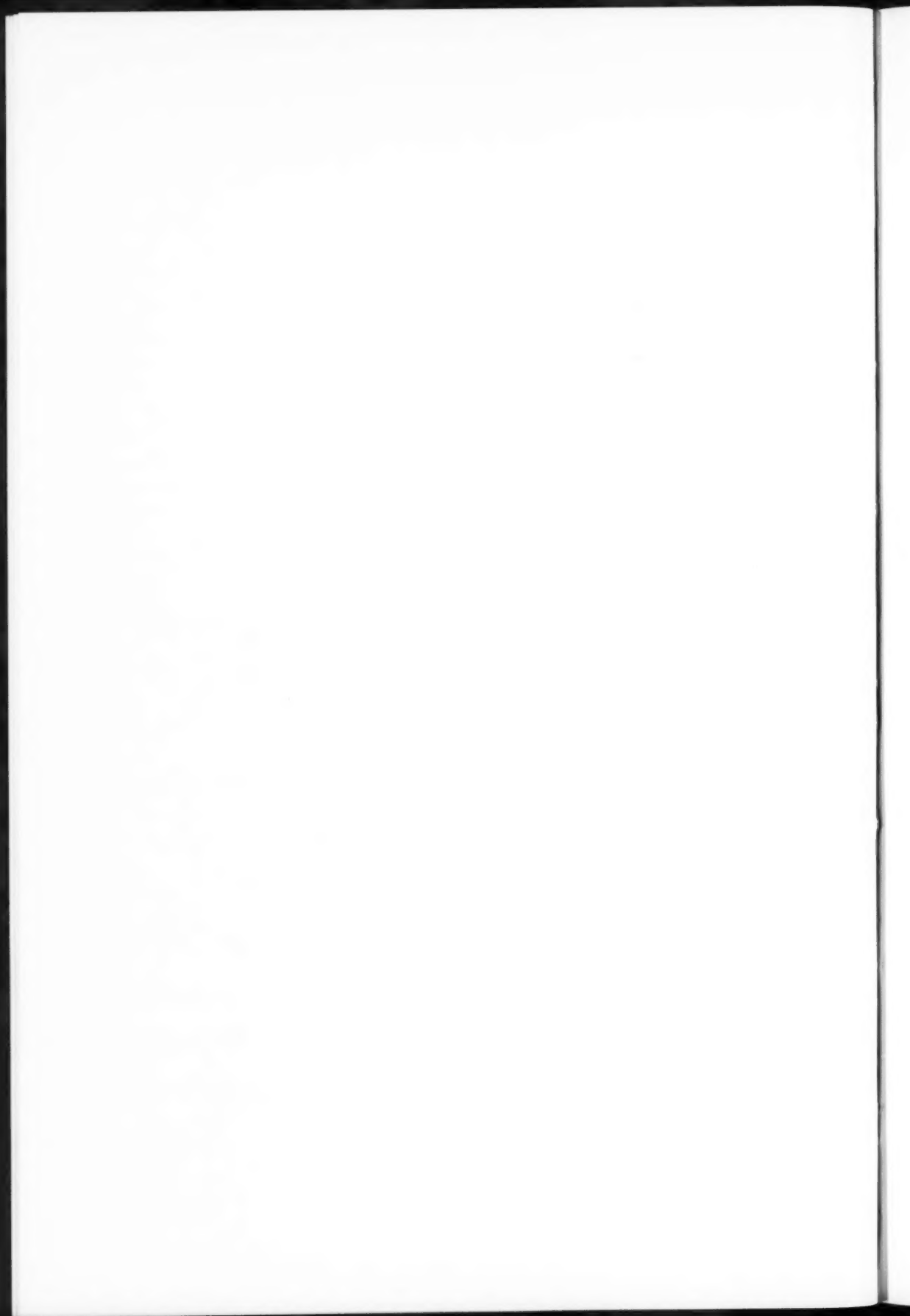
# PLATE IV



NOVA AQUILAE No. 3 (1918)

Direct photograph with 100-inch reflector, April 25, 1927. Exposure 45 min. on an Eastman 40 plate. Scale 1 mm = 2".

Slitless spectrogram with 100-inch reflector, August 2, 1926. Exposure 3 hrs. on an Eastman 40 plate. Two prisms and 3-inch camera.





reflector, with the use of two prisms and a 3-inch camera, show four distinct images of the envelope.  $\lambda 4686$  is the strongest and is perhaps twice as strong as the equally dense images in  $H\beta$ ,  $H\gamma$ , and  $H\delta$ . Faint traces of images appear in the region of  $N_1$  and of  $\lambda 4363$ .

A velocity of expansion of  $1''.0$  per year corresponds to a distance, in parsecs, of

$$D = 0.211r,$$

where  $r$  is the radial velocity, in kilometers per second, of the expanding shell relative to the central star. The radial velocity cannot be accurately measured on spectrograms obtainable at present, but reasonable values may be derived from the many high-dispersion spectra accumulated during the five or six months immediately following the outburst. The measures at Mount Wilson indicate that, after the systematic changes during the first month, the radial velocity, as derived from the displacements of metallic absorption lines, settled down to a fairly constant value of  $1650 \text{ km/sec.}$ <sup>1</sup> This velocity was maintained from July to November, 1918—as long, in fact, as the object could be followed with high dispersion. By the end of this period the envelope had already been detected and measured by Barnard.

The Balmer lines of hydrogen appeared as broad emission bands, the widths remaining approximately constant at least as late as March, 1919.<sup>2</sup> The velocities of approach and recession, as represented by the violet and the red ends of the bands, were about  $1750 \text{ km/sec.}$ <sup>3</sup> and hence of the same order as those derived from the absorption lines. Adams has suggested that the emission bands represent the expanding envelope and that the absorption lines arise from that portion directly in front of the star.<sup>3</sup>

<sup>1</sup> This result is derived from unpublished measures made at the Mount Wilson Observatory. See, in this connection, *Proceedings of the National Academy of Sciences*, **4**, 355, 1918.

<sup>2</sup> The Mount Wilson measures have not been published in detail, but, as a sample, those for the emission bands in February and March, 1919, may be found in *Publications of the Astronomical Society of the Pacific*, **31**, 183, 1919.

<sup>3</sup> *Mt. Wilson Communications*, No. 55; *Proceedings of the National Academy of Sciences*, **4**, 355, 1918; *Mt. Wilson Contr.*, No. 179; *Astrophysical Journal*, **51**, 121, 1920.

On this assumption, the radial velocity could be taken from either source. The larger values derived from the emission bands are more germane to the present problem, but the uncertainties involved in the measures suggest that the smaller but more precise values represented by the absorption lines may be a closer approximation to the actual conditions. The mean of the two, however, is a round number, 1700 km/sec., with an uncertainty of the order of 3 per cent, and this is sufficient for the purpose.

The corresponding distance<sup>1</sup> of Nova Aquilae No. 3, as derived from the formula given above, is

$$D = 360 \text{ parsecs ,}$$

$$\pi = 0''.0028 ,$$

$$m - M = 7.8 \text{ mag.}$$

The apparent magnitude of the star was about 10.5 before the outburst, and -1.4 at maximum. Hence, from an absolute magnitude of +2.7, it flared up to -9.2 and then slowly faded to its original luminosity. The diameter of the envelope is now about 6000 astronomical units, and is increasing at the rate of 360 units per year.

The results are consistent with the fact that the mean of the various trigonometric parallaxes, as determined by the photographic method, is small and negative. This indicates that the distance is very probably greater than 200 parsecs and hence that the linear velocity of expansion is greater than say 1000 km/sec.

CARNEGIE INSTITUTION OF WASHINGTON

MOUNT WILSON OBSERVATORY

April 1927

#### ADDENDUM

While the foregoing account of Nova Aquilae was in press, a 20-minute exposure on a fast plate, made by Milton Humason with the 100-inch reflector on July 20, 1922, came to our attention. No definite indications of a disk could be seen, but the size of the image relative to that of the diffraction pattern, when compared with other stars on the plate, suggested the possibility of a disk con-

<sup>1</sup> Lundmark, in 1922, stated that he had determined the parallax of Nova Aquilae No. 3 by this method, and that the result, 0.006, agreed exactly both with the mean of the three photographic parallaxes then available and with the value derived from the upsilon component of the proper motion (*Publications of the Astronomical Society of the Pacific*, 34, 210, 1922). He gives no further details.

cealed by over-exposure. When the plate was reduced by ferrocyanide, the supposition was confirmed; a sharp uniform disk was revealed about the central star.

The measured diameter of the original image,  $8''.8$ , is probably too large because of the over-exposure. The diameter after the reduction,  $7''.6$ , is believed to be too small because the narrow fringe of fainter nebulosity, apparent on the recent plates, was wiped out in the reduction. Although a nice accuracy in this matter is scarcely possible, it is significant that, on the obvious hypothesis of uniform expansion, the recent observations indicate a diameter for July, 1922, of  $8''.2$ , which is exactly midway between the extreme values representing measures before and after the reduction.

Humason's plate, therefore, is believed to be the earliest direct photograph on which the image is definitely recorded; and the diameter at that date was of the order of eight seconds of arc.

## REVIEWS

*Anregung von Quantensprüngen Durchstöße.* By F. FRANCK and P. JORDAN. Berlin: Julius Springer, 1926. Pp. 304. 51 figs. M 21.

This book forms the third volume in the series on "The Structure of Matter," edited by Born and Franck. After a discussion of the phenomena of free paths and electron collisions, the first half of the book is devoted to a review of the methods used for observing critical potentials and to a complete summary of the latest results. Later chapters discuss the probabilities of excitation and ionization at a collision, ionization by positive ions and by high temperatures, the life of excited atomic states, and collisions of the second kind. Then comes a summary of the work on the critical potentials of molecules and the relations of the theory of excited atomic states to photochemistry and chemical reactions. The subject matter is analyzed and discussed critically in a masterly manner, and very full references are given to the literature. The book is an excellent summary of the present state of our knowledge in this field, and will be welcomed by students and experimenters interested in this new and important branch of physics.

A. J. DEMPSTER

---

## ERRATA

Vol. 65, No. 4, May 1927, article on: "The Motions of Giant M Stars," by Gustaf Strömberg:

Page 241, in equ. (6) add the term  $-2\beta z\epsilon' \frac{d^2F_1}{dx_1^2}$

Page 253, in equ. (27), for  $\sqrt{\pi}\gamma$  read  $\gamma\sqrt{\pi}$

Page 254, in equ. (28), for  $\gamma_y$  read  $\gamma_4$  and for  $2\alpha\gamma_4$  read  $2\alpha\gamma_4$

Page 255, twelfth line from top, omit  $\pm$ .

Page 259, the wording of the quotation near the bottom of the page is inexact, although the meaning has not been changed.

Page 264, third line from top, for irregularities read singularities.

Page 264, seventh line from top, after the word "be," insert "to assume."

Page 265, twenty-first line from top, add at end of sentence, "and the actual cause of the asymmetry remains unexplained."